MEDICAL UNIVERSITY OF VIENNA

Christoph Dibiasi

Kinetik der Thrombusbildung

in Abhängigkeit von der Plasma-Fibrinogenkonzentration

Diplomarbeit

Medizinische Universität Wien
Department für Biomedizinische Forschung

Betreuerin: Ao. Univ. Prof. Dr. med. vet. Ursula Windberger, BSc

Wien, Juli 2017

Zusammenfassung

Einführung

Blut ist eine Suspension bestehend aus Zellen in flüssigem Plasma. Es besitzt die Fähigkeit, seinen Aggregatzustand zu verändern und einen festen Thrombus zu bilden. Der zentrale Schritt ist hierbei die Umwandlung des Plasmaproteins Fibrinogen in Fibrin, welches anschließend spontan polymerisiert.[1,2]. Die resultierende Änderung der Festigkeit des Blutes kann direkt gemessen werden, z.B. mittels Rotations-Thromboelastometrie (ROTEM).[3] Eine mögliche Alternative stellt die Oszillationsrheometrie dar, mit welcher Proben untersucht werden können, indem sie bei unterschiedlichen Frequenzen und Deformationsamplituden oszillatorisch geschert werden. Die Materialeigenschaften des Thrombus (z.B. das Speichermodul G′ als Maß für die Festigkeit) können hiermit umfangreicher charakterisiert werden.

Methodik

In dieser Diplomarbeit werden die mechanischen Eigenschaften von Blutproben gesunder Probanden bei unterschiedlichen Fibrinogenkonzentrationen mittels Rheometrie untersucht. Zuerst wird die Änderung u.a. der Parameter G′ and G″ (Verlustmodul) während der Blutgerinnung beobachtet. Im Anschluss werden die Veränderungen dieser Parameter bei steigender Scheramplitude untersucht. Auch ROTEM Messungen der entsprechenden Proben werden durchgeführt und mit den rheometrischen Messungen verglichen. Die Effekte der höheren Fibrinogenkonzentration werden desweiteren nicht nur quantitativ, sondern mittels Rasterelektronenmikroskopie auch morphologisch beschrieben.

Resultate

Sowohl mittels Rheometrie also auch mittels ROTEM zeigt sich eine schnellere Blutgerinnung sowie zu einer erhöhten Thrombusfestigkeit bei höheren Fibrinogenkonzentrationen. Morphologisch zeigen sich bei höherer Fibrinogenkonzentration dickere Fibrinfasern, eine Abnahme der Porengröße des Netzwerkes sowie eine Zunahme der Verzweigungen der Fasern.

Abstract

Introduction

Blood is a suspension of cellsembedded in plasma. In response to physiological and/or pathological triggers, it can change it's state and turn into a solid blood clot or thrombus. Quintessential to this process is the conversion of the plasmatic protein fibrinogen to fibrin, which spontaneously polymerises.[1,2] The resulting change in clot stiffness can be measured, for instance by rotational thromboelastometry (ROTEM).[3] A possible alternative to ROTEM is oscillatory shear rheometry, enabling more complex investigations of mechanical clot properties. In rheometry, samples are probed by subjecting them to oscillating shear at various frequences and/or deformation amplitudes. One of the core rheometric parameters is storage modulus G', which relates to clot stiffness.[4]

Methods

In this diploma thesis the mechanical properties of blood clots formed at different fibrinogen concentrations are investigated by rheometry by ROTEM. The change of G' (among other parameters, e.g. loss modulus G") is monitored during coagulation. After complete clot formation, a so-called amplitude sweep is conducted, in which the oscillation amplitude is increased and the resulting changes in G' and G" are measured. Additionally, visualisation of blood clots is performed using scanning electron microscopy.

Results

There is a strong positive correlation between fibrinogen concentration and clot viscoelatic parameters measured by rheometry and ROTEM: Blood clots made from blood with higher fibrinogen concentrations are produced significantly faster and exhibit increased stiffness. Morphological analysis by scanning electron microscopy shows that increasing fibrinogen concentration yields clots with thicker fibres, smaller pore sizes and greater branch point density.

Contents

1 Background

1.1 Blood coagulation

Human blood is an organ composed of cellular parts immersed in plasma. Normally, it's a fluid, however in a number of physiological (e.g. blood vessel injury) and pathological states (e.g. myocardial infarction, stroke or venous thrombosis) blood can transform its aggregate state into a solid one. This process is called haemostasis, coagulation or clotting, the end result of which is a stable blood clot attached to the site of vessel injury (or pathological triggering site). Blood clots consist out of thrombocytes and erythrocytes interconnected by a fibrous network made from the protein fibrin.

The understanding the coagulation process has been developed over the last century, but is not at all complete. Historically, clotting has been described to occur in two phases: primary hemostasis, in which a platelet clot is produced, and secondary hemostasis, in which fibrin fibres are formed between the platelets and thereby a stable network is built. Secondary hemostasis involves numerous proteins called clotting factors, which are present in plasma as inactive precursor proteins. During coagulation, clotting factors are activated in a positive feedback loop, which was described in breakthrough studies to act like a "cascade" or "waterfall"[5,6]. Clotting factors were traditionally divided in extrinsic and intrinsic pathway, both of which activate factors belonging to the common pathay and thereby lead to the ultimate goal of fibrin generation.

Despite its clinical usefulness, this model has some limitations: extrinsic and intrinsic pathways are not independent, but rather influence each other. Secondly, defects in the intrinsic pathways do not result in any relevant bleeding disorder.[7] These limitations were among the reasons for favouring an integrated model of clot formation, in which primary and secondary hemostasis are not said to occur separately, but rather intertwined.[1,8] Three phases of clotting are distinguished in the newer model: initiation, amplification and propagation.

1.1.1 Cellular haemostasis — Thrombocytes

Platelets or thrombocytes in their unactivated state are discoid cells with a diameter of 2 µm to 5 µm. They are divided off bone marrow megacariocytes and circulate in the blood until adhesion to the subendothelium (or a developing clot), activation and incorporation into a thrombus — a process, in which they are ultimately consumed. If no clot formation takes place, they are degredaded in the spleen after a lifetime of approximately 8 days.[9]

Adhesion

Thrombocytes carry several transmembrane receptors (table 1.1) to attach to subendothelial proteins like tissue factor (*TF*) and collagens: *GPVI* and *GPIa/IIa* and the most important one being GP *Ib-V-IX*. Its ligand is van Willebrand Factor (*vWF*), which functions as bridge to *TF* bearing structures. *GPVI* and *GPIa/IIa* both bind collagens without *vWF*. However, those receptors only facilitate weak adhesion. Only expression of integrin $\alpha_{IIb}\beta_3$, which occurs after platelet activation, guarantees strong enough attachment to the matrix to withstand blood flow.[1]

Activation

Multiple stimuli facilitate the activation process: Primarily, *GP Ib-V-IX* binding to a ligand induces weak platelet activation. Secondly, many soluble agonists are usually present at sites of injury while inhibiting substances like nitric oxide (*NO*) and prostacylcin (PGI_2) are missing due to endothelial defect. Furthermore, platelets are also capable of autocrine and paracrine activation by releasing several types of granulas with procoagulants.

Several actions are initiated by platelet activation and performed partly simultaneously:

- Granula secretion
- Integrin $\alpha_{IIb}\beta_3$ conformational change, which allows it to bind to its ligands.
- Shape change

Table 1.1: Selected thrombocyte receptors important for coagulation[1]

Receptor name	*Ligands*	*Function*
GPIb-V-IX	vWF	unstable adhesion and activation
GPVI	collagens	adhesion
GPIa/IIa (integrin $\alpha_2\beta_1$)	collagens	adhesion
GPIIb/IIIa (integrin $\alpha_{IIb}\beta_3$)	fibrinogen (main ligand), vWF, fibronectin	stable adhesion and aggregation
PAR1	thrombin	strong activation
PAR4	thrombin	strong activation
$PY2_{12}$	ADP	activation
TXA_2 receptor	TXA_2	activation
α_{2a}	epinephrine	weak activation
5-HT-R	serotonine	weak activation
	vasopressine	weak activation
	platelet activating factor (PAF)	activation

- Aggregation

Granula secretion

Platelets contain several intracellular compartments, among them α-granulas, which are most numerous, and dense granulas. Platelet activation leads to granula content secretion, thereby activating the thrombocyte more strongly (autocrine effect), but also attracting and activating additional platelets (paracrine effect).

α-granulas contain proteins synthesised in megakariocytes (e.g. *FV* and *vWF*) but also proteins acquired from blood plasma (e.g. fibrinogen). Among the contents of dense granulas are *ATP*, *ADP*, Ca^{2+} and serotonine.[9] Thrombocytes themselves can not synthesise proteins due to their lack of a cell nucleus.

Shape change

Activated platelets initially change their shape from discoid to spherical and then gradually express longitudinal protrusions.[10] The reason for this processs is the rearrangement of the intracellular cytoskeleton, composed of actin, in response to increased intracellular Ca^{2+} concentrations due to activation.

Aggregation

To impact blood flow on a macroscale, the thrombus has to grow and firmly attach other platelets as well as erythrocytes to the existing structure. Integrin $\alpha_{IIb}\beta_3$ is the most important platelet surface receptor facilitating attachment of additional platelets. Its most important ligand is fibrinogen. After conversion to fibrin, fibers form and link platelets to the fibrin network.[1]

The importance of integrin $\alpha_{IIb}\beta_3$ highlighted by patients with missing or afunctional receptors, a bleeding disorder termed *Glanzmann thrombasthenia*.[11] Integrin $\alpha_{IIb}\beta_3$ inhibitors are very potent disruptors of clot formation. They are used clinically in high risk patients with acute coronary syndrom, but are also associated with high bleeding risks.[12]

Retraction

Fibrinogen bound to integrin $\alpha_{IIb}\beta_3$ gets converted to fibrin during plasmatic coagulation and thus platelets are incorporated into the fibrin mesh. Contractile force generated by intracellular platelet myosin-actin interaction is transmitted to the fibrin mesh. This process takes places early in coagulation and generates tensile stress on fibrin fibres[13], thereby increasing clot stiffness and changing fibre direction.[14]

The physiological reason for clot retraction remains unclear, however it has been proposed that retraction facilates wound closure by pulling together the wound edges and that blood vessel obstruction is reduced by decreasing the clot volume.[15]

1.1.2 Plasmatic coagulation — How to form a clot

1.1.2.1 Initiation phase

Blood vessel injury imposes *TF*, which not only acts as ligand to platelet membrane receptors (see above), but also kicks off plasmatic coagulation: Circulating *FVIIa* forms a complex with *TF*, which activate both factor *FIX* and *FX*.

FXa uses *FVa* as cofactor to make up the membrane-bound *prothrombinase complex*, which activates prothrombin (*FII*) to thrombin (*FIIa*).[1]

The initiation phase is localised at cell membranes of matrix cells expressing *TF*. Once *FXa* dissociates from the cell surface, it is promptly inhibited by tissue factor pathway inhibitor (*TFPI*) and antithrombin (*AT*). This mechanism prevents uncontrolled thrombus spreading away from the point of injury. However, *FIIa* is not membrane bound and diffuses away from the subendothelium, thereby starting the next coagulation phase.

1.1.2.2 Amplification phase

By the mechanism discussed so far, only small amounts of thrombin are generated, which don't suffice for the conversion of fibrinogen to fibrin. However, *FIIa* activates several other factors (*FV*, *FVIII*, *FXI*) and thereby starts a positive feedback loop, the end result is an increased *FII* turnover to *FIIa*.

1.1.2.3 Propagation phase

Prothrombinase activity — located on the platelet surface — is enhanced by the *tenase complex*, which consists of *FIXa* and *FVIIIa*. Turnover of *FIX* activation to *FIXa* is enhanced by *FXIa* (boosted itself by *FIIa*). During propagation phase, thrombin concentration is increased high enough to proteolyse fibrinogen (*FI*) to fibrin (*FIa*).

It's important to realise, that prothrombinase serves two different purposes in initiation and propagation phases: During initiation, it's located on the surface of *TF* exposing cells and mereley kicks off the positive feedback loop by making a small

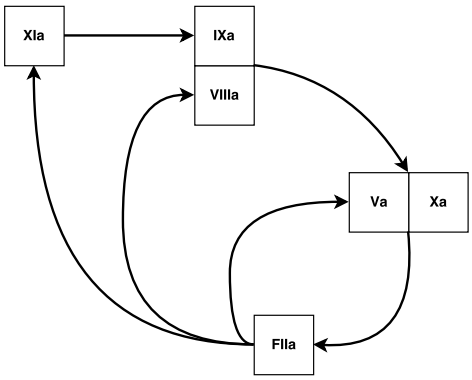

Figure 1.1: *FIIa* activity is increased in a positive feedback loop

amount of thrombin, which dissociates from *TF* bearing cells and attaches at platelet surfaces. Afterwards, platelet bound prothrombinase concentration increases (stimulated by tenase) and produces a massive amount of thrombin — enough to cleave fibrinogen.

1.1.2.4 Fibrinogen conversion

The key reaction of coagulation is the conversion of fibrinogen to fibrin. Fibrinogen is a dimer synthesised in hepatic cells. Each half consists out of three polypeptide chains (Aα, Bβ, γ).[16]

It is converted to fibrin monomers by proteolytic cutting of fibrinopeptides A and B and thereby exposing A and B "knob" regions. Fibrin monomers then form oligomers by binding of knob A and B to complementary "holes" a and b of another monomer. Physiologically, interaction of A knob-holes is more important with the role of B knob-hole interaction remaining unknown. Using this knob-hole interaction mechanism, two fibrin molecules connect to each other in a staggered manner with a periodicity of 22.5 nm.[16]

By the same mechanism, fibrin oligomers grow longitudinally and form protofibrils, which are two-stranded chains of fibrin monomers. Protofibrils also aggregate laterally to generate fibres, which are initally floppy, but are interlinked by *FXIII* (which is also activated by thrombin).

1.1.3 Fibrinolysis

After physiological vessel healing the clot is no longer needed and gets removed. As with coagulation, this process is also fine tuned and involves numerous molecules. The central point is the activation of the zymogen plasminogen to plasmin, which degrades fibrin and thereby dissolves the clot.

Two serine proteases can activate plasminogen: tissue plasminogen activator (*tPA*) and urinary plasminogen activator (*uPA*). *tPA* is released continously by blood vessel epithelial cells, but most of it is bound to plasminogen activator inhibitor 1 (*PAI-1*). Free *tPA* can activate plasminogen to plasmin. The catalytic effiency of *tPA* very much depends on the presence of fibrin — by this means plasmin production is locally limited to the clot site. While *tPA* is thought to be mainly involved in hemostasis, *uPA* seems to be important in extravascular processes (i.e. wound healing). Correspondingly it is mainly produced by fibroblasts and urinary epithelial cells (from which it was initially purified) and doesn't require fibrin as cofactor.[17]

Plasmin is a hepatic serine protease can break down fibrinogen, dissolved fibrin and crosslinked fibrin. Different degradation products originate from this process depending on the substrate, the clinically most important being the *D-dimer*.[17] Several inhibitors confine fibrinolysis and restrict it to the site of the blood clot:[18]

- Plasminogen activator inhibitor 1 (*PAI-1*) and 2 (*PAI-2*), which inactivate *tPA* and *uPA*
- α2-antiplasmin which binds and inactivates free plasmin. Plasmin bound to fibrin is spared (another mechanism localising fibrinolysis to thrombi)
- Thrombin activated fibrinolysis inhibitor (*TAFI*) which modifies fibrin to decrease it's ability to bind plasmin and therefore slows down fibrinolysis

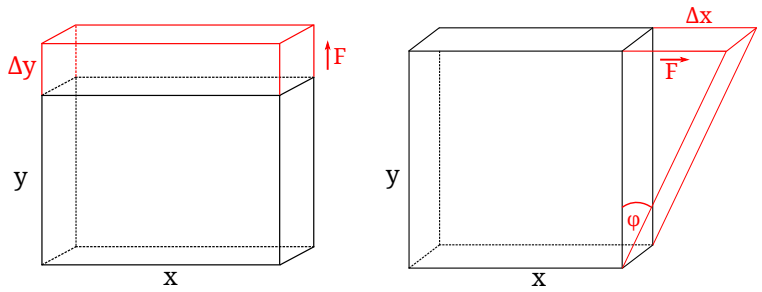

Figure 1.2: Normal strain (in this case: pulling) and shear strain differ in the direction of the force vector

1.2 Viscoelasticity

To completely understand the behavior of blood clots in response to deformations in vivo (e.g. by blood flow) and in vitro (e.g. by rheometry) deformations it is necessary to clearly define the underlying physical principles. Blood clots, like many other biological materials (i.e. muscle, cartilage or bone) show visceolastic behavior to various degrees.[19]

1.2.1 Elasticity and plasticity

Elasticity can be defined as "tendency of a solid material to return to its original shape after being deformed"[20]. The opposite of elasticity is *plasticity*. Plastic deformations are permanent after the deforming force has been removed. Elastic-plastic behavior occurs when a sample returns partly to its original state after deformation, but some permanent deformation remains.

1.2.1.1 Normal stress and strain

Applying an external force (i.e. pushing, pulling, cutting) to an object causes deformation. This deformation is quantified as strain ϵ. Taking in regard only one axis, strain is defined as the change of length in relation to the original length (figure 1.2):

$$\epsilon = \frac{\Delta y}{y_0} \tag{1.1}$$

Straining an object causes internal forces to manifest, which are referred to as *stress*. Uniaxial normal stress σ is defined as force F, which is normal on surface A within the body. It is given in pascal (Pa).

$$\sigma = \frac{F}{A} \tag{1.2}$$

Strain and stress are related to each other. This relationship is expressed by the elastic modulus. When refering to normal strain, it is called Young's modulus E:

$$E = \frac{\sigma}{\epsilon} \tag{1.3}$$

The elastic modulus is a material constant. Rigid materials have high elastic moduli while soft materials have low elastic moduli.

1.2.1.2 Shear stress and strain

Shearing deformation forces are applied tangential to a material's surface. While the principle discussed in the previous section is the same, shearing strain is defined somewhat differently (figure 1.2). Shearing strain γ is the ratio of displacement in one direction to the perpendicular axis caused by a tangential force.

$$\gamma = \frac{\Delta x}{y} \tag{1.4}$$

The definition of shear stress τ doesn't differ from normal stress. However, the direction of the internal force F is *parallel* to the surface A.

$$\tau = \frac{F}{A} \tag{1.5}$$

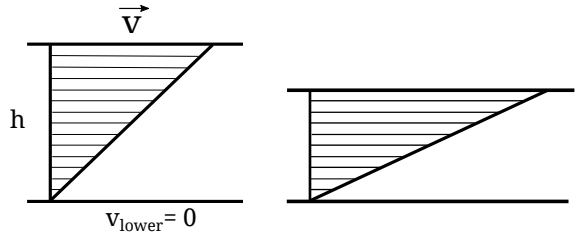

Figure 1.3: Shear rate $\dot{\gamma}$ is proportional to the speed of the upper plate v and inversly proportional to the distance between the plates h. Correspondingly, the setup on the left yields a lower shear rate than the one on the right, while plate velocity v is the same.

The elastic modulus is called shearing modulus G. It gives information on how easy it is to shear a material.

$$G = \frac{\tau}{\gamma} \tag{1.6}$$

Shear rate $\dot{\gamma}$ is the rate at which shearing strain is applied to the material. It is defined in a two plate model shown in figure 1.3: A fluid is flowing at constant velocity between two plates with infinite area.The upper plate is moving with velocity v while the lower remains stationary ($v = 0$). In order to satisfy the so-called no-slip condition, fluid adhesion to the plates is assumed to be greater than than fluid cohesion. Strain rate $\dot{\gamma}$ is the ratio of movement speed of the upper plate v to the distance between the two plates h. This implies, if the speed of the upper plate is increasing, or the plate distance is descreasing, $\dot{\gamma}$ will increase as well.

$$\dot{\gamma} = \frac{v}{y} \tag{1.7}$$

1.2.1.3 Linear and non-linear elastic behavior

Whether a material shows elastic or plastic response to deformation depends on the magnitude of the strain applied. Many materials exhibit a linear stress response only to small strains up to the so-called *yield point* or *elastic limit*, which marks the beginning of the nonlinear elastic range, in which the deformation applied is (at

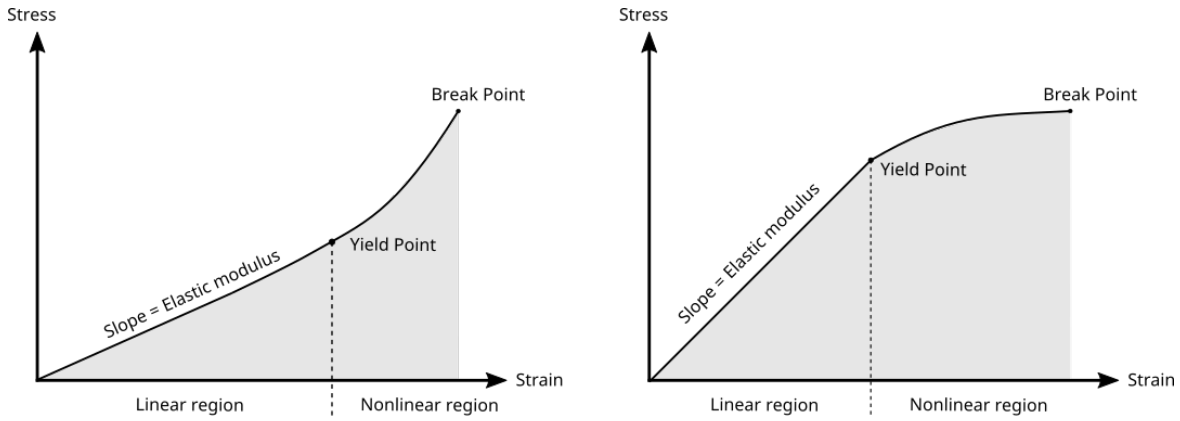

Figure 1.4: Strain-stress diagram. Many materials exhibit linear elastic behavior only at small strains. The slope of the curve in the linear elastic range equals the elastic modulus (either E or G depending on the direction of applied strain). At higher strain amplitudes (above the yield point) the relationship between strain and stress turns disproportional and materials can show stiffening (left) or softening (right) behavior.

least partly) permanent. If strain is increased even further, the break point of the material is reached.

Material behavior in the nonlinear range is either softening, which makes further deformation easier to perform (as indicated by an reduced elastic modulus), or stiffening, which leads to an increased elastic modulus and thus, to higher resistance against deformation. As opposed to synthetic polymers, many biological materials and biopolymers show strain stiffening behavior, for instance gels made from fibrin[16,21,22], collagen[23] or the cytoskeletal protein actin[24,25,26].

Strain stiffening in biological materials is believed to prevent deformations which cause structural damage to the material.[23] Skin for instance shows strain stiffening: If it's pulled only slightly, skin is easily deformed. However, increasing the normal deformation beyond the yield point requires higher force due to an increased elastic modulus. If skin didn't exhibit strain stiffening, normal strain at higher amplitudes could lead to rupturing.

1.2.2 Viscosity

Viscosity η is a material property of fluids that describes the resistance to deformation. In laminar flow, viscosity is caused by internal friction between adjacent fluid layers. This internal friction is determined by the solvent componentsand also strongly on temperature: most fluids exhibit higher viscosity at lower temperature.

When subjected to the same driving force (i.e. pressure difference), low viscosity fluids flow faster than high viscosity fluids.[27,28] This is described in Hagen-Poisseuille's law:

$$Q = \Delta p \frac{\pi r^4}{8\eta l} \tag{1.8}$$

Viscosity is dependent on shear stress τ and shear rate $\dot{\gamma}$:

$$\eta = \frac{\tau}{\dot{\gamma}} \tag{1.9}$$

The viscosity of blood for instance is strongly dependent on the haematocrite. To maintain constant systemic perfusion Q in diseases with increased haematocrite the heart work has to be increased. Additionally, vessel wall shear stress τ increases as well.[28]

Equation 1.9 can be transformed to it's general form, called Newton's law. It states that:

$$\tau = \eta \cdot \dot{\gamma} \tag{1.10}$$

Fluids which obey the constitutive equation 1.10 are called Newtonian fluids (i.e. water or blood plasma). However in many fluids, η and $\dot{\gamma}$ exhibit no linear relationship. Those non-Newtonian fluids can either be shear thickening ($\eta \propto \dot{\gamma}$) or shear thinning ($\eta \propto \frac{1}{\dot{\gamma}}$).

An example for non-Newtonian fluids is blood, which shows shear thinning behavior (descrease of η as $\dot{\gamma}$ is increased). This is mainly attributed to the reversible formation of red cell aggregates, which dissamble at higher shear stresses.[29]

1.2.3 Putting it together: Viscoelasticity

Biological materials often exhibit a mixture of elastic and viscous behavior: They are *viscoelastic*. The difference between elastic, plastic and viscoelastic phenomena can be illustrated by slightly indenting e.g. an rubber play ball with one's finger (and thereby exercising deformation strain γ). Upon removement of the finger, a purely elastic ball would immediately return to it's original shape. If the ball was hypothetically made from a completely viscous material, it would remain deformed indefinitely. A viscoelastic rubber ball would return to it's original form after some delay.

Viscoelastic materials are characterised by complete reversibility of applied strain[1], but with delay in stress response after after strain application and removal (figure 1.5). Nearly all materials display some kind of viscoelasticity, however at very different extents, which often make it difficult to recognise viscoelastic behaviour as such.

Three aspects of viscoelastic behaviour are described in this section:

1. Hysteresis (material behavior in load-unload cycles)
2. Creep (material response to constant stress application)
3. Stress relaxation (material response to constant strain application)

Hysteresis

In contrast to purely elastic materials, the strain-stress diagrams of visceolastic samples display different progressions for loading and unloading cyles, a phenomenon termed "hysteresis". The area under the curve corresponds to energy disspitated during deformation. The more fluid samples are, they feature higher energy dissipation and larger areas under the curve. In elastic samples on the other hand, there are smaller areas under the curve corresponding to their elasticity, because the energy raised during deformation is reused for restoring the original state during unloading.

[1] as long as the strain amplitude remains below the yield point

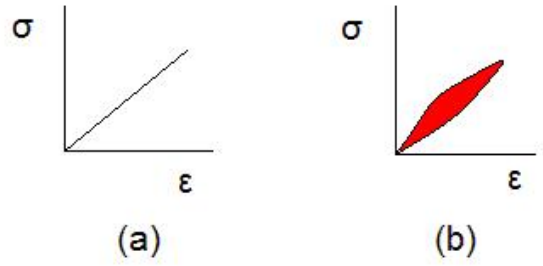

Figure 1.5: Strain-stress diagrams illustrating purely elastic behavior (left) and hysteresis in viscoelastic substances (right)

Creep

Creep refers to the time dependent change in strain when materials are subjected to constant stress (figure 1.6a).[19] At small stress magnitudes, induced strain is still in the linear range and strain is reversible after stress unloading. At higher stress levels (or if stress is maintained for a longer period), strain increase can lead to permanent deformation or material destruction.

Stress relaxation

Stress relaxation is the time dependent decrease of material stress in response to constant strain exposure (figure 1.6b).

Purely elastic bodies exhibit no stress relaxation as stress is always proportional to strain. Purely viscous substances on the other hand feature instant stress relaxation (stress impulse response).[27] Both cases are extreme behaviors. Viscoelastic substance show stress relaxation with gradual decrease of stress in response to constant strain, the extent of which is dependent on material composition.[19] Viscoelastic fluids will approach zero stress, while in viscoelastic solids stress falls off to a plateau level, the height of which is governed by the elastic properties of the material.[4]

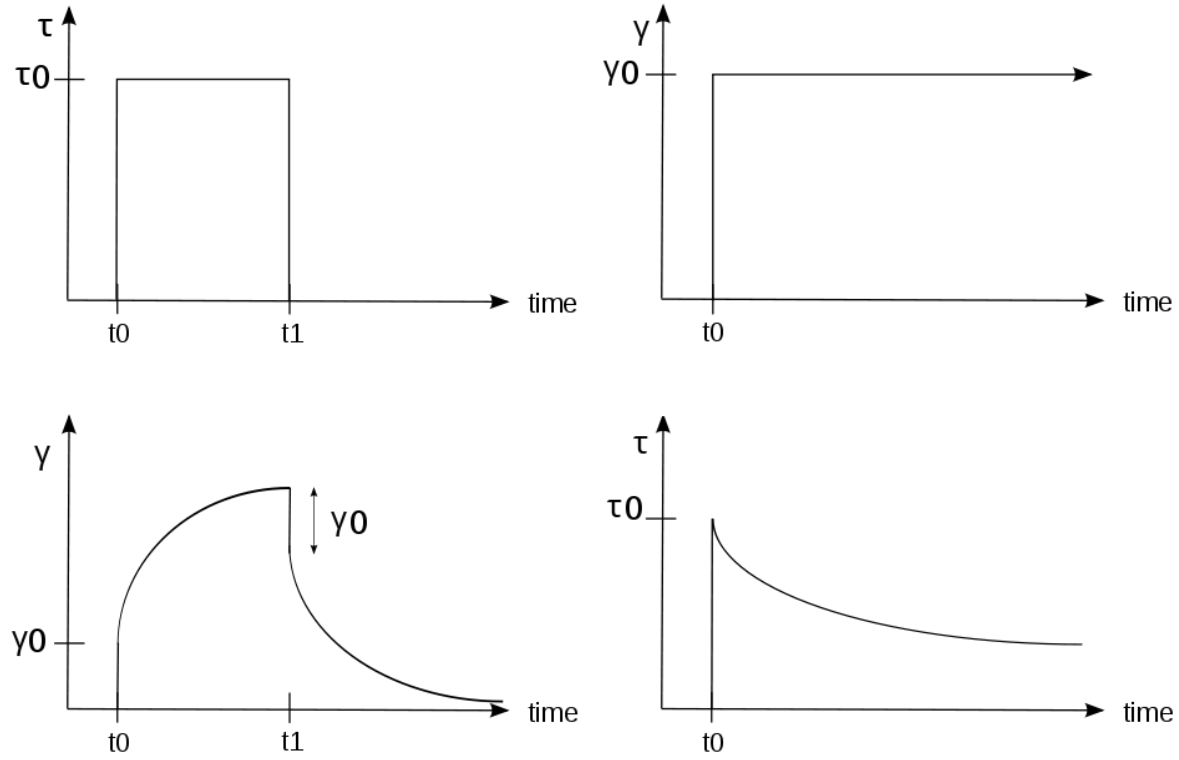

(a) (b)

Figure 1.6: Creep and stress relaxation are time dependent changes of stress/strain in viscoelastic materials after subjection to strain/stress.

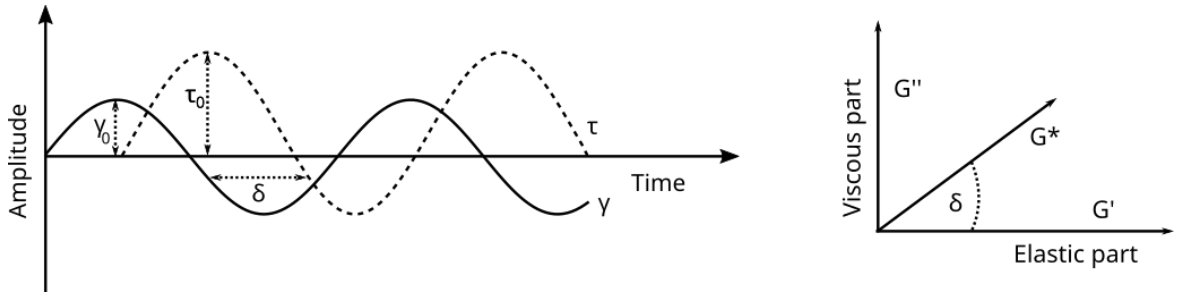

Figure 1.7: Complex moduli are obtained by subjecting samples to oscillation strain and measuring stress response.

1.2.4 Dynamic mechanical analysis

Materials can not only be probed by stepwise strain and stress application, but also by imposing oscillating strain or stress (figure 1.7).[2]

Imposed strain is dependent on maximum strain amplitude γ_0 and angular frequency ω. The resulting stress is recorded by the measurement device (i.e. rheometer) and can be modelled as sinus function shifted by phase angle δ, provided that strain applied is in the linear viscoelastic range.

$$\gamma(t) = \gamma_0 \sin(t\omega) \tag{1.11}$$

$$\tau(t) = \tau_0 \sin(t\omega + \delta) \tag{1.12}$$

Phase angle δ can be interpreted as delay of stress response to deformation. It is considered a material property. In purely elastic materials, strain and stress curves are in phase ($\delta = 0°$) while purely viscous materials exhibit a maximum phase difference of $\delta = 90\ °$. Viscoelastic materials show a phase difference depending on the magnitude of their elastic and viscous properties.

The relationship of τ and γ is the same for oscillatory strain — however the elastic modulus is not a scalar but the complex number G^* (called complex or dynamic shear modulus).

$$\tau(t) = G^* \cdot \gamma(t) \tag{1.13}$$

$$G^* = G' + i \cdot G'' \tag{1.14}$$

Like the scalar shear modulus G, G^* it is defined as the ratio of strain to stress:

$$G^* = \frac{\tau(t)}{\gamma(t)} \tag{1.15}$$

G^* can also be defined geometrically as vector with the components G′ and G″

[2] In principle, it's possible to impose strain or stress interchangeably and to measure the other variable. Because in this diploma thesis measurements were conducted strain controlled, the explanations here are limited to imposing oscillating strain.

Table 1.2: Characterisation of different materials adapted from[4]

ideally viscous	*VE liquid*	*VE material at GP*	*VE solid*	*ideally elastic*
Newtown's law	Kelvin/Voigt model		Maxwell model	Hooke's law
$\delta = 90°$	$90° > \delta > 45°$	$\delta = 90°$	$45° > \delta > 0°$	$\delta = 0°$
$\tan(\delta) \to \infty$	$\tan(\delta) > 1$	$\tan(\delta) = 1$	$\tan(\delta) < 1$	$\tan(\delta) \to 0$
$G' \to 0$	$G'' > G'$	$G' = G''$	$G' > G''$	$G'' \to 0$

VE...viscoelastic, GP...gel point

(figure 1.7):

$$G' = \frac{\tau_0}{\gamma_0} \cdot \cos(\delta) \tag{1.16}$$

$$G'' = \frac{\tau_0}{\gamma_0} \cdot \sin(\delta) \tag{1.17}$$

Storage modulus G′ can be interpreted as the amount of deformation energy that is stored inside the material during strain application. This energy is used after strain reversal to restore the original state of the material. G' corresponds to the elastic properties of the material.

Loss modulus G'' is the part of deformation energy, which dissipates during strain application. After strain reversal this energy cannot be used for restoration of the material originals state. Therefore, not purely elastic materials ($G'' > 0$) will not be able to restore its original state fully.

Viscoelastic materials are defined by the combination of both G′ and G″ (table 1.2). Elastic and viscous moduli are however not fixed, but can vary depending on temperature, already applied strain/stress or over the time. One example is gelation (e.g. cooking of marmelade or curing of resins), in which G′ increases and becomes larger than G″: the sample transitions from a viscoelastic fluid to a viscoelastic solid. The transitioning point or *gel point* is of special interest. It can be defined as time point where $G' = G''$.[4]

1.2.5 Linear and nonlinear viscoelasticity

Definition of G' and G'' depends on the assumption that measured $\tau(t)$ is a sinusoidal wave. This assumption holds only in the linear viscoelastic range. Once γ is increased sufficiently, plastic deformation occurs and $\tau(t)$ deviates from a pure sinus function. The definition of G' and G'' (and other derived parameters) are dependent on the assumption, that $\gamma(t)$ and $\tau(t)$ are sinus functions, so G′ and G″ (which are automatically calculated by the user software) are not absolutely valid. Rather, more sophisticated analysis methods, like large shear oscillating rheometry (LAOS), have to be utilised, which is beyond the scope of this diploma thesis.[30]

However, while the absolute values of G′ and G″ may be distorted, they can still be used as good approximation.[4]

1.3 Rheometry

Viscoelastic behavior is examined by applying oscillating shear strain to samples in a *dynamic shear rheometer*. There are also other rheometers available (i.e. extensional rheometers), which are not covered in this section.

A dynamic shear rheometer consists out of a measurement geometry, temperature control element and high precision motors and sensors for controlling movement of the measurement geometry in shear and axial direction. An appropriate computer software is used for setting up and operating the device.

1.3.1 Shear movement motor

Usually, one part of the measurement geometry is moving while the other one remains stationary. The movement is generated by a electric motor. Two basic parameters govern it's operation: Torque M and deflection angle φ. Either one can be defined in the rheometer software by setting maximum shear stress amplitude τ_0 (controlled shear stress mode [CSS]) or maximum shear deformation amplitude γ_0 (controlled shear deformation mode [CSD]). The corresponding free variable depends on the intrinsic properties of the sample measured.

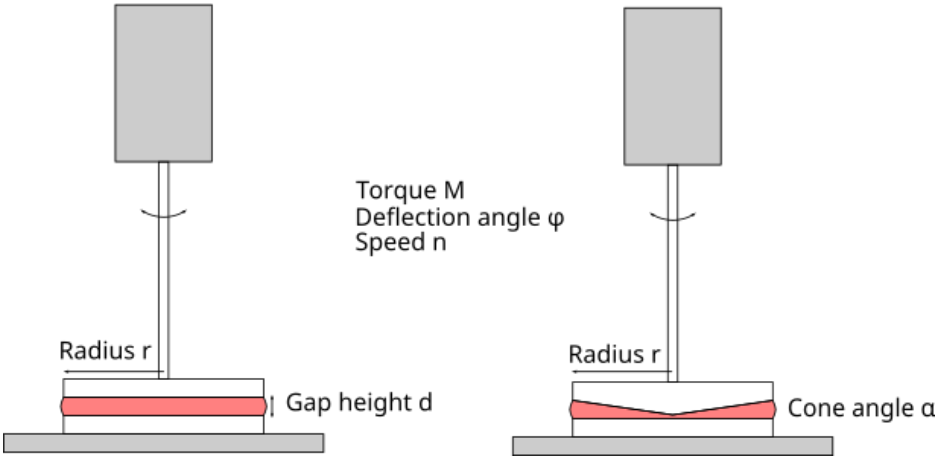

Figure 1.8: Parallel plates and cone-plate measurement geometries

Set τ_0 and γ_0 can be directly translated to M and φ and vice versa by using measurment geometry specific conversion factors. Some rheometers also allow direct measurment of rotational speed n which translates to shear rate $\dot{\gamma}$.

1.3.2 Axial movement motor

The measurement chamber parts need to be movable in order to (1) allow sample placement and cleaning and (2) to modify the height of measurement gap, which influences the shear rate $\dot{\gamma}$ (equation 1.7). Some rheometers are also equipped with a normal force F_n sensor, which can be used to detect positve or negative pressures in the sample chamber or alternatively adjust the gap height on the fly if the sample volume changes during the measurement (i.e. by evaporation).

1.3.3 Measurement chamber

For illustration of rheological measurments the variables where defined in section 1.2.1.2 using a simple model of two plates. (Couette model). In practise, simple *translational* shear is not applicable because of the undefined behavior at the edges. To overcome this, *rotational* displacement is utilised. Different measurement geometries are are available and the choice depends on sample characteristics.

All rheological variables introduced so far where defined for Couette flow. If different methods are used, they are to be redefined. Because only the plate-plate measurement unit was used for this work, the others are only covered briefly.

1.3.3.1 Parallel plate

The sample is placed between two parallel circular plates with radius r and gap width h. The sample volume required is given by $V = \pi r^2 h$. The upper plate is oscillating with set frequency. The amount of deflection is dependent on whether the rheometer is set to CSD or CSS mode: In CSD mode, the deformation amplitude is fixed. In CSS mode, the oscillation stops once the set amount of shear stress is recogniced by the device.

One limitation of the parallel plates setup is non uniform share rate distribution across the plate surface: Shear rate $\dot{\gamma}$ is highest at the edge and decreases to $\dot{\gamma} = 0$ at the center. Other possible problems are sample slippage over the plate borders or evaporation of the sample, both leading to wrong viscoelastic parameters.

1.3.3.2 Cone-plate

This measurement system consists out of a lower stationary plate and an upper cone with a cone angle α and radius r. The cone is not directly positionend on the lower plate, but at a distance h. In contrast to the parallel plate setup, it ensures an uniform shear rate distribution. However, not all samples can be analysed in the cone-plate setup: Suspensions with particle sizes greater than the gap height are not appropriate.

1.3.3.3 Coaxial cylinders

This measurement unit consists out of an outer hollow cylinder (cup) with another cylinder embedded into it. The axes of both cylinders line up (= coaxial). Provided a sufficiently small gap between both cylinders, the setup translates directly to the Couette flow model.

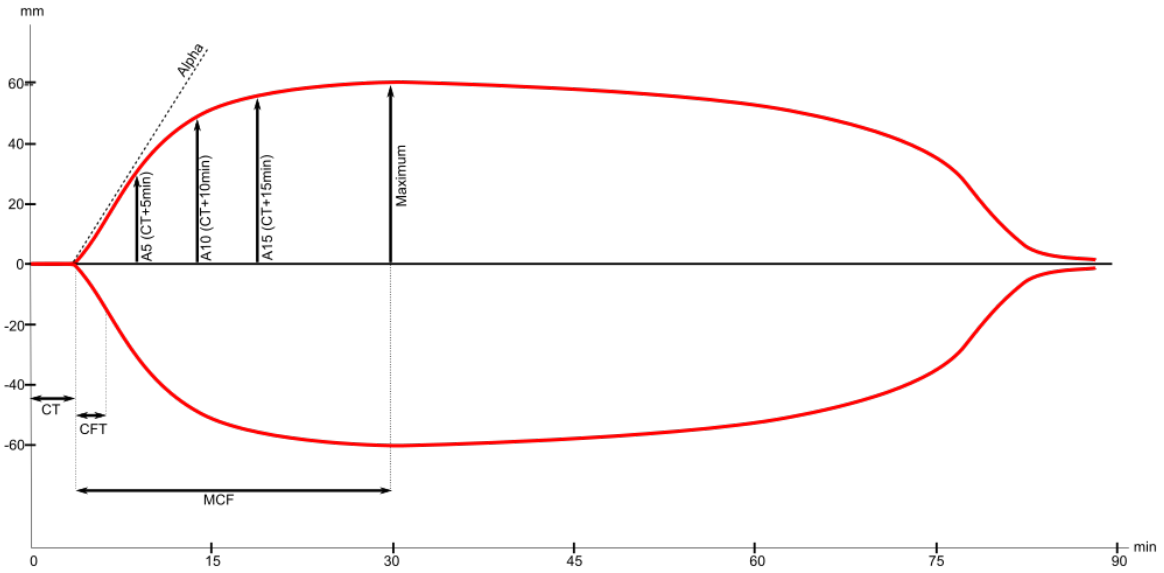

Figure 1.9: Annotated TEMogram with definition of most important thromboelastometric parameters.

There are two modes of operation: *Searle* mode for which the inner cylinder is moving and *Couette mode*, in which the cup is moving.

1.4 Rotational-Thromboelastometry (ROTEM)

Rotational-Thromboelastometry (ROTEM) is a point-of-care-test for assessing different aspects of haemostasis. A low volume whole blood sample is placed in a cup and an oscillating pin is inserted. Due to the coagulating blood, the pin movement is getting more and more impaired, which is detected by a light sensor and plotted over time (figure **??** and figure 1.9). ROTEM therefore mimicks a rheometer with a coaxial cylinder measurment device, but focuses on ease of use.

Several distinctive phases are described in the so called TEMogram: (1) Inital clot development (clotting time CT_{ROTEM} [seconds])[3], in which the pin moves freely and no movement restriction is detected. (2) Clot formation, during which pin oscillation is increasingly impaired as the clot strength increases. Three variables

[3]Originally only named CT, however to differentiate between clotting times measured by rheometry and ROTEM, in this diploma thesis appropriate suffixes are added.

describe this phase: Clot formation time (CFT [seconds]), which is defined as time span beginning at CT_{ROTEM}, until an arbitrary clot amplitude of 20 mm is detected. Maximum clot firmness (MCF [mm]) and time to MCF (MCF-t [seconds]) refer to the maximum of pin movement restriction. (3) It is claimed that clot lysis is also detected in ROTEM. Pin restriction and thus, amplitude in the TEMogram are decreasing in this phase. The lysis index at minute 30 after CT (LI_{30} [%]) and maximum lysis (ML [%]) quantify this behavior.

Different activators of coagulation can be used in order to assess different aspects of haemostatic. In NATEM mode just Ca^{2+} and no activator is added to the citrated blood sample. To investigate functioning of the extrinsic pathway, tissue factor is used as activator in EXTEM mode. The intrinsic pathway can be assed in INTEM (activator: kaolinite) or HEPTEM (activator: kaolinite and heparinase) mode. Using the platelet inhibitor cytochalasin D and an extrinsic activator in FIBTEM mode, fibrinogen impact on clot formation can be viewed independently.

ROTEM is used in the perioperative assessement assement of the coagulation system to guide hemostatic therapy[3] or the transfusion of allogenic blood products.[31]

1.5 Viscoelasticity of coagulating blood

During clotting, blood changes from a viscoelastic liquid into a viscoelastic solid. This is a gelation process — correspondingly, loss modulus G″ decreases while storage modulus G′ increases (figure 1.10).

Measured clot properties (i.e. G′ and G″) and clot ultrastructre are highly dependent not only on the environmental conditions during coagulation but also on the concentrations of the blood components involved:

The most important positive predictor of final clot stiffness is the sample fibrinogen concentration. This was shown in numerous studies utilising rheometry[32,33] and ROTEM[34,35,36] on whole blood sample, blood plasma samples[37,38] and fibrin gels[39,21]. Fibrinogen concentration and/or functionality can be impaired due to heredetary defects or in acquired states[40,41] (e.g. liver disease or traumatic coagulopathy[42]), which negatively affects the haemostatic function.

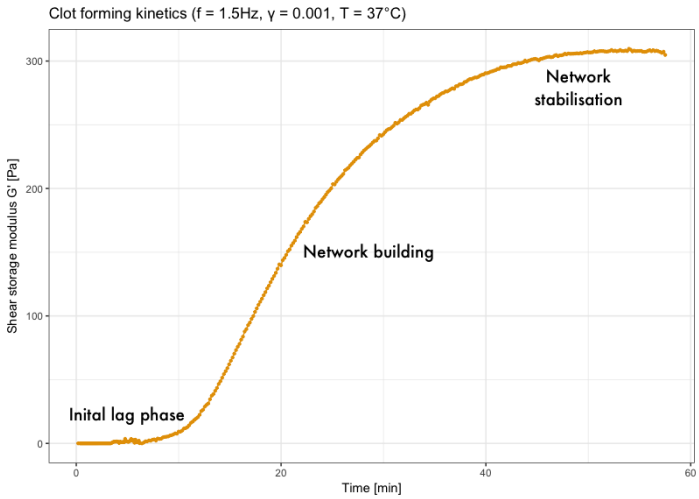

Figure 1.10: Three clotting phases can be distinguished: (1) inital lag phase, in which the biochemical reactions described above leading to high enough thrombin activity, (2) network building phase, in which enough thrombin is present to facilitate fibrinogen cleavage and polymerisation. After consumption of all available fibrinogen, complete fibre formation and crosslinking (3) network plateau phase occurs.

The kinetics of fibrinogen cleavage, which depend on thrombin availability, govern fibrin polymerisation. Low concentrations favor a low fibre count with fibres becoming thicker and exhibiting less branch points and greater pore size.[40] Fibre crosslinking is facilitated by *FXIIIa* and increases clot stiffness at protofibril and fibre level.[43,39]

As the fibre mesh is formed, red blood cells are entrapped, which decreases clot stiffness. Rising RBC concentrations are therefore associated with weaker clots.[44,45,46] Another important parameter is thrombocyte concentration: Platelet are positioned at central fibre branching points and perform blood clot retraction by pulling at the fibres. This is though to increase clot stiffness.[15,47,48]

2 Aims of the project

The main goal of this diploma thesis was to determine the impact of increased plasma fibrinogen concentration in whole blood clots on (1) clot forming kinetics and on (2) the viscoelastic properties in response to increased shear deformation.

Samples were to be measured by rhemoetry and rheometric clot kinetics data was to be compared with corresponding parameters measured by ROTEM. In principle, there should be no gross differences in data related to clot forming kinetics, as the measuring techniques are closely related. However, it could be possible that rheometry is more sensitive due to the ability to fine-tune measurement parameters.

Additionally, clots formed at different plasma fibrinogen concentrations were to be analysed morphologically. It is known that fibrin network structure changes remarkibly during coagulation[49], is dependent on erythrocyte concentration[45] and is altered in thrombotic states.[50,51]

Studies investigating mechanical properties of the coagulation system very often only utilise either fibrin solutions or plasma, either with or without platelets. Because it is known that erythrocyte concentration significantly alters clot stiffness[45], there is clearly a need for mechanical analysis of whole blood clots.

Using full blood as sample material comes with technical difficulties like correct phlebotomy, handling and storing of blood samples. Interindividual differences have to be taken into account and make measurements considerably more difficult to interpret as opposed to samples which consist out of clearly defined volumes of the necessary chemicals. Having this in mind, this diploma thesis can also be seen as a first step towards addressing those technical difficulties of using whole blood.

3 Methods & Material

3.1 Subjects

This study was approved by the ethical review commitee of the Medical University of Vienna (EK No. 1371/2015). Nine subjects were recruited. Requirements for inclusion were (1) being healthy according to the classification of the American Society of Anaesthesiology, (2) no occurence of abnormal bleedings and (3) no reported intake of medication known to alter haemostasis in the last 7 days.

After receiving informed consent, one peripheral venous blood collection was performed on each subject at the Department of Anaesthesiology of the University clinic of Vienna.

3.2 Sample preparation

9 mL blood was drawn from the antecubital vein using a 21 G Vacuette® butterfly needle and a Vacuette® vacutainer system with citrate solution (3.8 %) for anticoagulation (Greiner Bio-One GmbH, Kremsmünster, Austria).

We had defined three sample groups: the first with native fibrinogen level (BL), the second with slightly elevated fibrinogen level (MED) and the third with substantially elevated fibriogen level (HIGH).

BL samples were left unaltered, whereas for MED and HIGH approximately 50 mg, respectively 100 mg fibrinogen were directly added. Gentle tilting of the sample tube was applied to improve the dissolution process.

All samples were stored at room temperature until further processing with a maximum storage time of 4 h.

Of each sample, aliquots were analysed at the Institute of Laboratory Medicine at the Medical University of Vienna to acquire a full blood count, the fibrinogen concentration according to Clauss[52], the aPTT and quick value.

3.3 Rheometry

The rheometer "Physica MCR 302" (Anton Paar, Graz, Austria) equipped with a plate-plate measurement system (diameter 25 mm) with roughened surface ("PP25/P3").

After careful mixing of the test tube, 0.58 mL was taken from the sample, mixed with 38.5 µL 0.2M Ca^{2+} solution and was put immediately into the rheometer to start the measurement. The temperature of the reaction chamber was set to 37 °C and gap width d was set to 1 mm.

The device was operated in controlled shear deformation (CSD) mode. For the time sweep, oscillation with deformation amplitude γ_0 set to 0.001 % and frequency f set to 1.5 Hz was performed until establishment of the G' plateau. Immediately afterwards, the amplitude sweep was started — with the sample left in situ — with γ_0 set to increase logarithmically from 0.001 % to 300 %.

3.4 Thromboelastometry

The "ROTEM DELTA" (TEM International, München, Deutschland) device was used, according to the manufacturers instructions, to measure blood clotting at 37 °C for two hours in NATEM mode.

3.5 Data recording & processing

For each measurement, the data presented in table 3.1 was recorded. Continuous data (G', G" and F_n) for both, time and amplitude sweep, was analysed using a custom computer program written in Python 3.6.1. Data points were interpolated using spline regression to remove gross outliers and smooth the curve. Time sweep data was processed to find CT_{rheo}, G'_{max} and G'_{max}. CT_{rheo} was operationally defined as first time point, where G' is greater than 10 Pa. The remaining parameters mentioned in table 3.1C were defined intuitively. Amplitude sweep data was analysed to find local G' minima and maxima corresponding to shear softening and stiffening. Representative program output is shown in figure 3.1 and 3.2.

Table 3.1: Data collected for each sample

General		
sample type	[BL, MED, HIGH]	
erythrocyte concentration	$[10^{12}L^{-1}]$	
haematocrit	[%]	
haemoglobin	$[g\,dl^{-1}]$	
thrombocyte concentration	$[10^{9}L^{-1}]$	
leukocyte concentration	$[10^{9}L^{-1}]$	
fibrinogen concentration	$[g\,l^{-1}]$	
Collected by rheometry continuously through the whole measurement[a]		
shear storage modulus	G'	[Pa]
shear loss modulus	G''	[Pa]
normal force	F_n	[N]
Collected by rheometry		
clotting time	CT_{rheo}	[minutes]
maximum shear storage modulus	G'_{max}	[Pa]
time to maximum shear storage modulus	G'_{max}-t	[minutes]
minimum normal force	F_{min}	[nN]
maximum normal force	F_{max}	[nN]
normal force range	F_{range}	[nN]
G′ at deformation $\gamma = 0.1$[b]	G'_{LVE}	[Pa]
γ at softest point	$\gamma_{softest}$	[1]
G′ at softest point	$G'_{softest}$	[Pa]
γ at stiffest point	$\gamma_{stiffest}$	[1]
G′ at stiffest point	$G'_{stiffest}$	[Pa]
(D) **Collected by ROTEM**		
clotting time	CT	[minutes]
clot formation time	CFT	[minutes]
maximal clot firmness	MCF	[mm]
time to maximal clot firmness	MCF-t	[minutes]
maximum lysis	ML	[%]
area under the curve	AUC	[1]

[a] For time and amplitude sweep separately
[b] Operationally defined as strain still in linear viscoelastic range

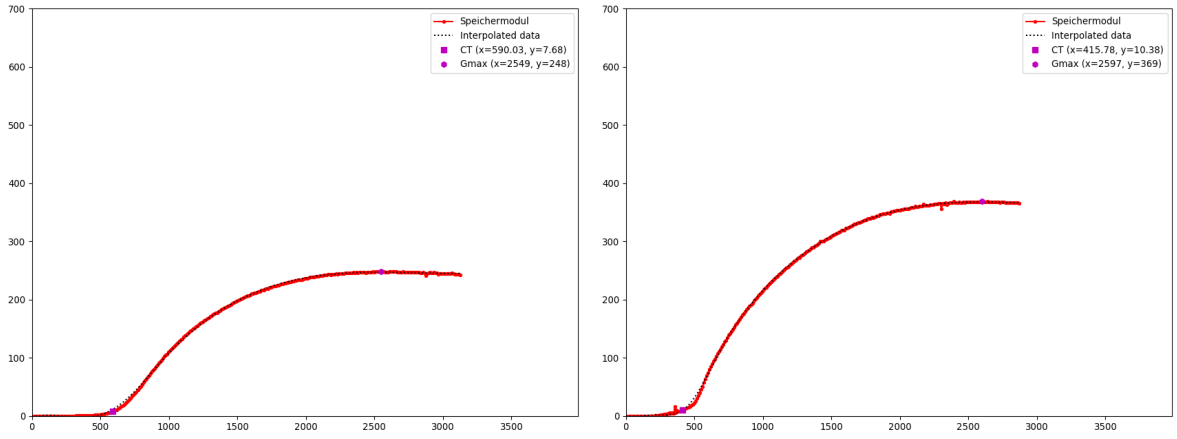

(a) (b)

Figure 3.1: Exemplary output of the custom computer program used to analyse time sweep data. After spline regression of raw data points, CT_{rheo}, G'_{max} and G'_{max}-t are detected by the program. Pictures shown are BL (a) and MED (b) samples from the same subjects.

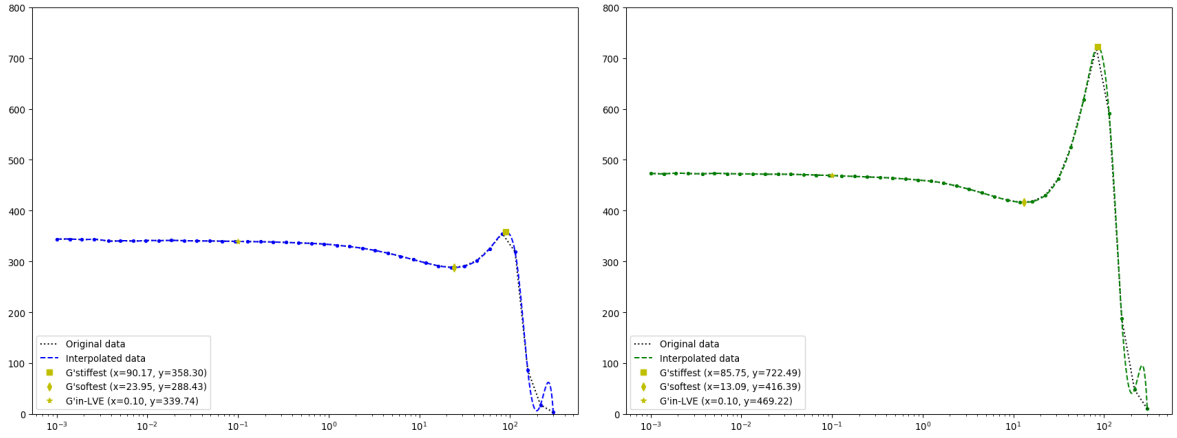

(a) (b)

Figure 3.2: Exemplary output of the custom computer program used to analyse amplitude sweep data. Whole blood clot exhibit complex shear softening/stiffening behaviour when shear strain is increased. Data points were interpolated using spline regression and local minima and maxima were detected. Pictures shown are BL (a) and HIGH (b) samples from the same subjects.

4 Results

Statistical analysis and data visualisation was performed using R version 3.4.0.[53]

4.1 Blood sample analysis

Table 4.1: Haematological parameters in the sample groups

		BL	Med	High
Erythrocytes	$10^{12}\mathrm{L}^{-1}$	4.92 ± 0.29	4.29 ± 0.45	
Haemoglobin	$\mathrm{g\,dL}^{-1}$	14.59 ± 0.70	12.93 ± 1.46	
Haematocrite	%	42.58 ± 1.72	37.53 ± 4.36	
Leucocytes	$10^{9}\mathrm{L}^{-1}$	6.59 ± 1.64	5.91 ± 2.28	
Thrombocytes	$10^{9}\mathrm{L}^{-1}$	282.00 ± 83.52	61.86 ± 40.98	
Fibrinogen	$\mathrm{mg\,dL}^{-1}$	253.89 ± 45.49	597.00 ± 184.56	811.50 ± 281.98

Values are given as mean $\pm$ standard deviation.
Due to experimential limitations, full blood count could not be performed for HIGH samples.

Statistical testing using two sided paired t-tests showed significant differences between BL and MED groups: $t = 3.78, p = 0.01$ for erythrocyte concentration, $t = 0.73, p = 0.49$ for leucocyte concentration and $t = 8.92, p < 0.001$ for thrombocyte concentration.

Fibrinogen concentration was raised significantly, as determined by one sided paired t-tests: $t = -6.60, p < 0.001$ for BL vs. MED comparison and $t = -3.865, p = 0.006$ for MED vs. HIGH.

4.2 Rheometry

Summary data is presented in table 4.2.

Table 4.2: Descriptive analysis[a] of rheometric and ROTEM parameters in the three sample groups

Rheometry (time sweep)		BL	MED	HIGH	ρ^b
CT_{rheo}	[s]	630 ± 66	411 ± 100	294 ± 80	-0.65^{**}
G'_{max}	[Pa]	282 ± 27	446 ± 81	543 ± 98	0.68^{**}
G'_{max}-t	[s]	2832 ± 366	2310 ± 256	1941 ± 179	-0.63^{**}
Fn_{min}	[nN]	-91 ± 19	-101 ± 13	-104 ± 21	
Fn_{max}	[nN]	-42 ± 20	-43 ± 9	-45 ± 6	
Fn_{range}	[nN]	50 ± 6	58 ± 14	59 ± 17	$0.11^{n.s.}$
Rheometry (amplitude sweep)					
G'_{LVE}	[Pa]	279 ± 33	427 ± 74	510 ± 87	
$\gamma_{stiffest}$	[%]	74 ± 15	77 ± 10	76 ± 2	$0.08^{n.s.}$
$\tau_{stiffest}$	[Pa]	201 ± 68	459 ± 80	681 ± 102	0.83^{**}
$G'_{stiffest}$	[Pa]	278 ± 62	628 ± 107	847 ± 115	0.83^{**}
$\gamma_{softest}$	[%]	27 ± 11	13 ± 4	10 ± 3	-0.64^{**}
$\tau_{softest}$	[Pa]	60 ± 19	47 ± 16	46 ± 15	-0.50^{*}
$G'_{softest}$	[Pa]	232 ± 37	381 ± 67	454 ± 73	0.64^{**}
G′-rel.stiffening	[%]	-3 ± 17	31 ± 11	40 ± 8	0.77^{**}
G′-rel.softening	[%]	-21 ± 10	-12 ± 3	-12 ± 3	0.44^{*}
G′-stiffening-span	[%]	119 ± 11	166 ± 24	188 ± 21	0.89^{**}
ROTEM					
CT	[s]	957 ± 131	516 ± 67	382 ± 92	-0.68^{**}
CFT	[s]	360 ± 60	123 ± 20	76 ± 8	-0.78^{**}
MCF	[mm]	48 ± 5	64 ± 4	67 ± 3	0.77^{**}
MCF-t	[s]	219 ± 118	1620 ± 203	142 ± 203	-0.77^{**}
ML	[%]	14 ± 4	14 ± 4	12 ± 5	
AUC	[1]	4702 ± 385	6312 ± 409	6558 ± 297	

[a] Values are rounded to integers and given as mean ± standard deviation.
[b] Pearson's correlation coefficient for corresponding variable vs. plasma fibrinogen concentration
[n.s.] not significant
[*] $p < 0.01$
[**] $p < 0.001$

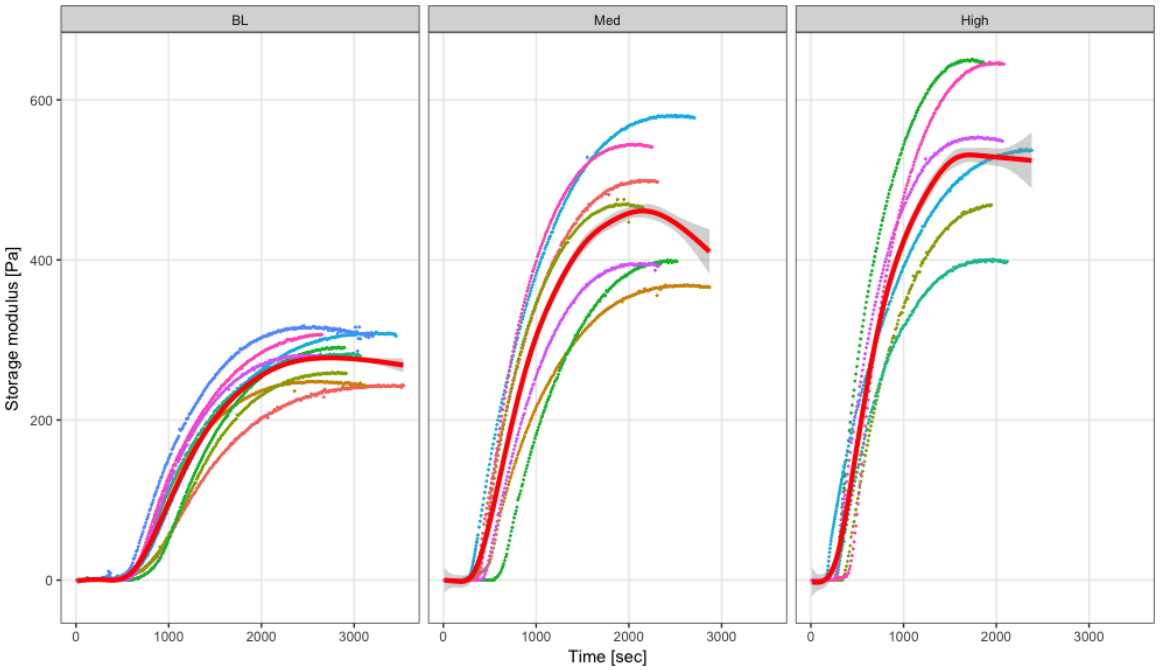

Figure 4.1: Average G′ increase (thick red line) determined by regression analysis for BL, MED and HIGH samples seperately. The individual measurements are shown as well.

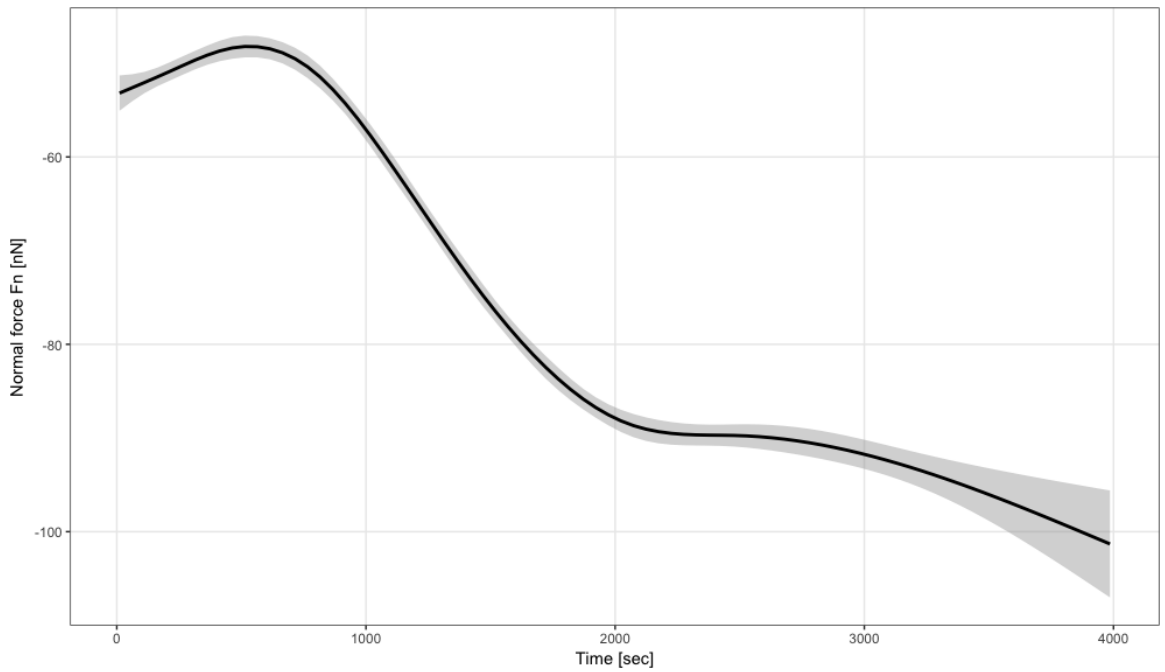

Figure 4.2: Average normal force development over course of coagulation (calculated using regression analysis of all measurements)

4.2.1 Coagulation kinetics

As described in section 1.5, G′ increases during coagulation with three different phases distinguishable (figure 1.10). Onset of coagulation (CT_{rheo}), G'_{max} and G'_{max}-t are strongly dependent on plasma fibrinogen concentration. Increasing fibrinogen yields faster clot development, an increased rate of G′ rise, a stiffer clot and decreased time until maximum stiffness is reached. These finding are also present in ROTEM measurements.

During coagulation, G″ increases as well, however it's a magnitude lower than G′ at all times, indicating that the sample is mostly solid. However, G″ measurement is much more unstable than G′.

Normal force F_n development is complex: Immediately after starting the measurement, F_n is slightly negative, then rises to slightly less negative values and after some time, decreases again and reaches more negative values. This behaviour is not dependent on fibrinogen concentration, with no significant differences between

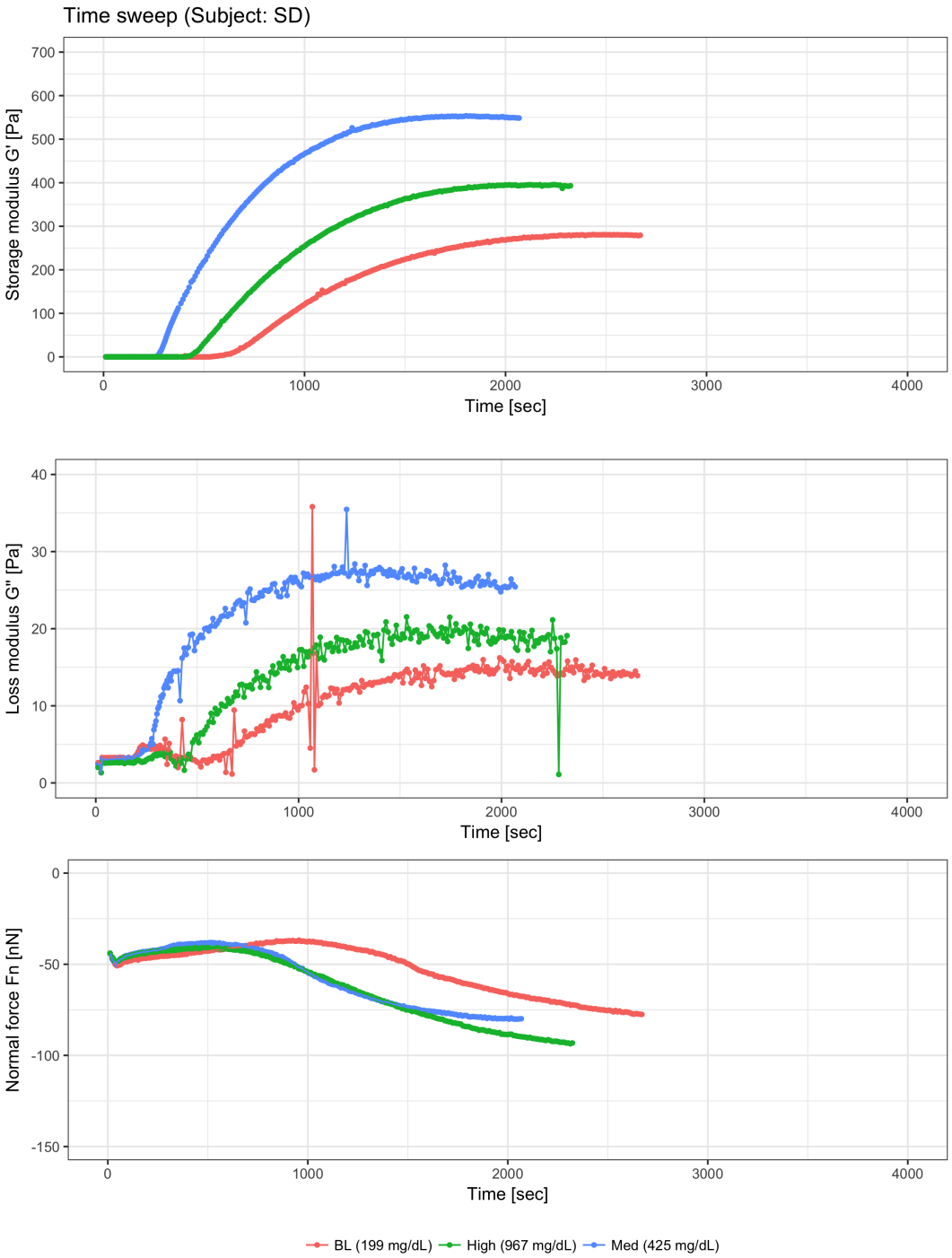

Figure 4.3: Representative time sweep measurement with G′, G″ and F_n development shown over the course of coagulation at different fibrinogen levels (BL 199 mg dl^{-1}, MED 425 mg dl^{-1}) and HIGH 967 mg dl^{-1}.

sample groups and an insignificant, low correlation coefficient of plasma fibrinogen concentration with F_n ($\rho = 0.11$).

4.2.2 Amplitude sweep results

Fully developed clots exhibit a complex, two phase response to logarithmically increased strain ranging from 0.001 % to 300 %. At small deformation amplitudes, approximately up to 0.5 %, G′ and G″ are constant[1], which is indicative of linear viscoelasticity.

At higher deformation amplitudes, a small decrease of G′ occurs, indicating minimal material softening. The minimum G′ value in this phase is refered to $G_{softest}$. As deformation amplitude is further increased, G′ rises again and thereby the clot displays shear stiffening behaviour.

After a peak G′ value (termed $G_{stiffest}$) is reached, the internal structure of the clot is destroyed and G′ as well as G″ decrease to zero.

4.3 ROTEM

Summary ROTEM data is shown in table 4.2. CT, CFT, MCF and MCF-t correlate significantly with plasma fibrinogen concentration.

Clotting time measured by rheometry (CT_{rheo}) is significantly reduced (paired two sided t-test with $t = -5.96, p < 0.001$), while G'_{max}-t is significantly higher than MCF-t (paired two sided t-test with $t = 14.14, p < 0.001$).

Comparison of G'_{max} and MCF using t-tests is not feasable due to different units of measurements. However, there was significant correlation between those two parameters: $\rho = 0.87, p < 0.001$.

[1] Ignoring small G″ derivation at very low deformations, which are attributed to erroneous measurement.

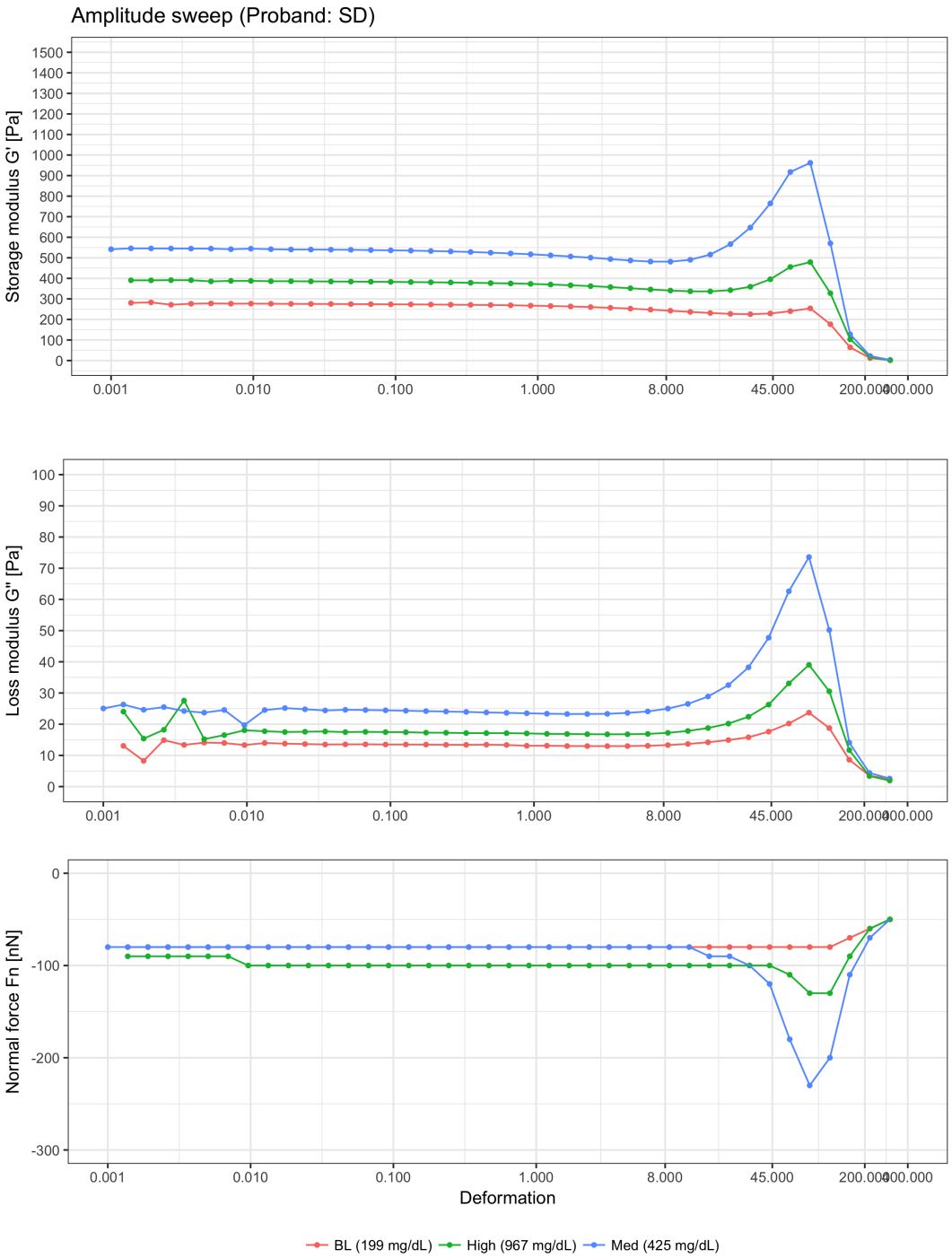

Figure 4.4: Representative amplitude sweep with G′, G″ and F_n development shown as shear strain is logarithmically increased at different fibrinogen levels (BL 199 mg dl^{-1}, MED 425 mg dl^{-1}) and HIGH 967 mg dl^{-1}.

4.4 Scanning electron microscopy

Selected clots were fixated and prepared for SEM visualisiation. Along with representative pictures, the relevant findings are described here.

Upper clot surfaces consist out of a fibrin network with trapped erythrocytes and platelets at major branch points. Minor branching takes place between the fibres. Morphological features of clots with higher fibrinogen concentrations include increased fibre diameter and higher branch point number and thus higher network density (figures 4.5 and 4.6). Another feature of MED and HIGH clots is the formation of mat like structures (fibrin mats).

Lower surfaces of BL clots show different structurisation: Only single fibres without any network formation and many loose erythrocytes can be seen (figure 4.7a and 4.7b). In HIGH samples, a thick and very dense layer of protein spans over the lower surface (not pictured).

Additionally, clot cutting and inspection of cross sectional surfaces was performed and also showed an layered clot organisation: The presence of a fibre network in the upper areas of the blood clot and unconnected, however tightly packed erythrocytes and debris in the bottom areas (of the BL clots, not pictured). In HIGH clots was also the thick opaque layer visible at the very bottom of the clot (figure 4.7c and 4.7d).

No morphological differences were found between central and peripheral areas (not pictured).

Interpretation of these findings is discussed in section 5.2.2.

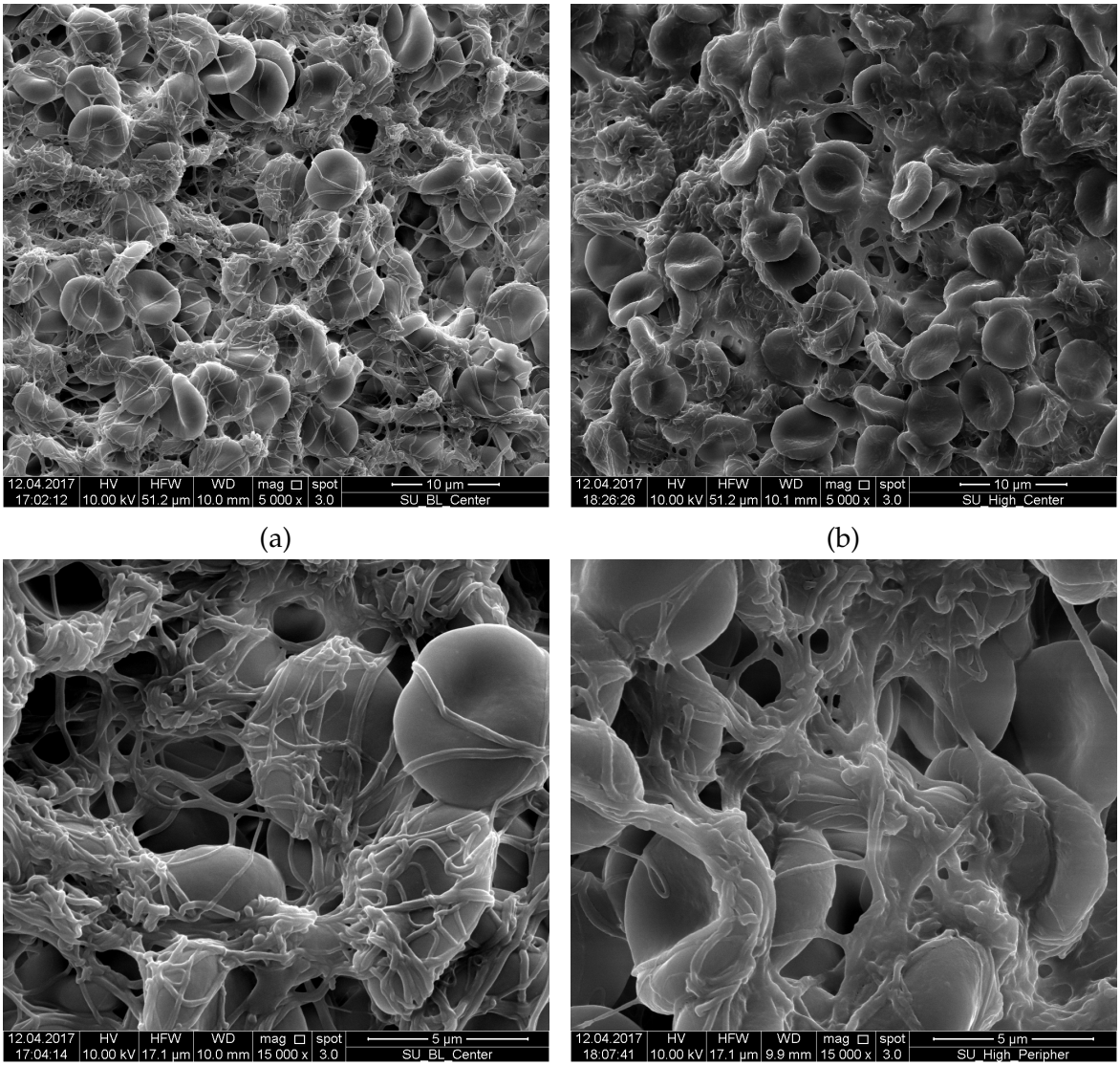

(a) (b)

(c) (d)

Figure 4.5: Clot surface overview pictures of BL (a, c) and HIGH blood clots (b, d). The fibrin network with incorporation of erythrocytes and platelet can be seen. Samples with higher fibringen concentration show thicker fibres and also mat like structures.
Magnification: 5000 × (a, b) and 15 000 × (c, d)

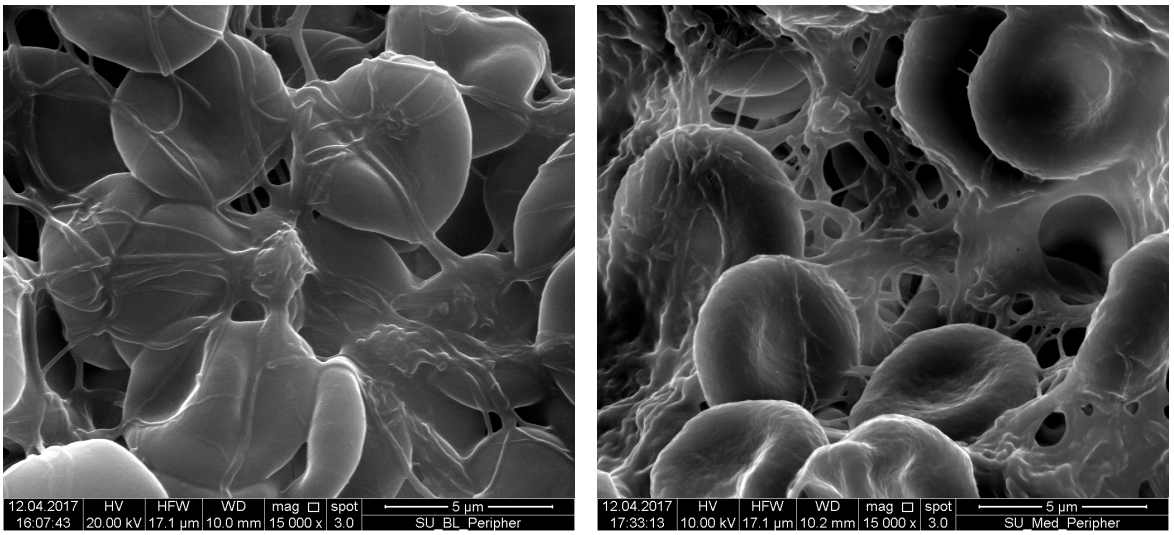

(a) (b)

Figure 4.6: Representative SEM pictures comparing BL and HIGH samples at 15 000 × magnification. Depicted in the center are activated platelet with fibres radiating out of it and thereby connecting the fibrin network to force generating platelets. Fibres in the HIGH sample show increased diameter and branch point density.

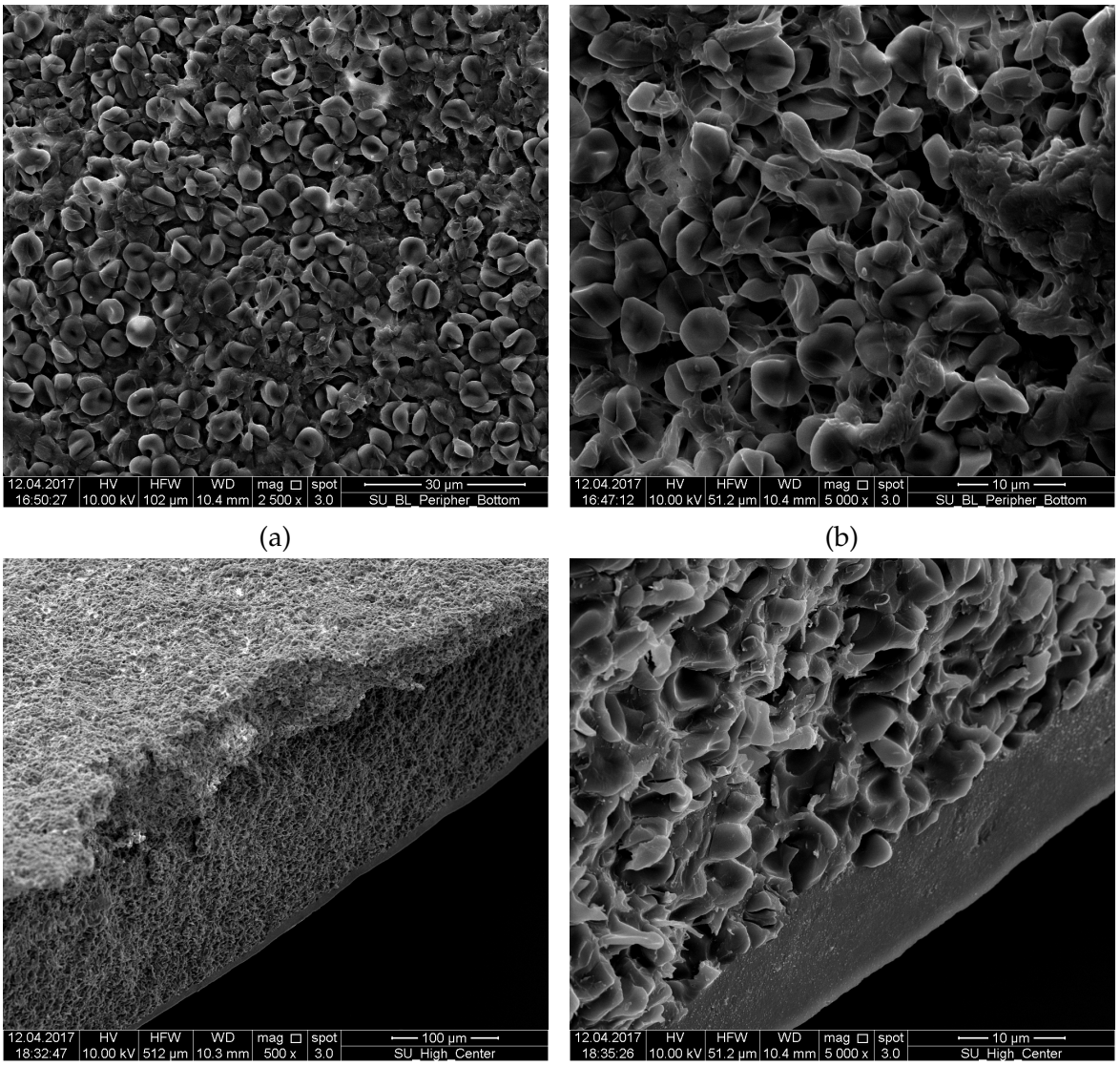

Figure 4.7: Three dimensional clot composition: Pictures (a) and (b) are taken the bottom of a BL clot (2500 ×, respectively 5000 × magnification). In contrast to figure 4.5a, the fibrin network seen is very loose or not even present at all. Pictures (c) and (d) show the cross sectional area of a HIGH blood sample (500 × and 5000 × magnification). Three distinct areas can be seen in (c): an upper layer with a fibre network like the one shown in figures 4.5 and 4.6. The middle layer consists out of compacted erythrocytes and debris. The lower layer is a very dense, homogenous structure without clearly visible cellular parts, possible related to the increased fibrinogen concentration.

5 Discussion

5.1 Conclusions

5.1.1 Clot forming kinetics

Increasing fibrinogen concentration leads to faster blood clot formation and increased stiffness. Morphological clot analysis by scanning electron microscopy revealed corresponding structural changes.

Rheometric clot parameters show good agreement with ROTEM. The high correlation coefficient of MCF vs. G'_{max} corresponds to findings of Solomon *et al.*[54] and Sølbeck *et al.*[55]. Although only an operational definition of clotting time was applied in this diploma thesis, blood clotting was detected significantly earlier by rheometry than by ROTEM. Additionally, G'_{max}-t was significantly higher than corresponding MCF-t. This findings could indicate that rheometry provides a more accurate way of measuring mechanic clot properties. Whether increased accuracy is of clinical relevance remains subject of further studies.

5.1.2 Non-linear clot behaviour

The complex softening-stiffening response for whole blood clots is — to the knowledge of the author — described here for the first time. It is however known that fibrin gels, PRP and PPP clots show strain stiffening[39,23,37], the origin of which is not fully discovered.

Recently, it was shown by Piechocka *et al.* that fibrin gels exhibit a triphasic shear stiffening response: Initially, as fibers straighten out, there is a linear viscoelastic response. Afterwards shear stiffening occurs at individual fiber level and at last, at network level. Indeed, a triphasic response is observed in this diploma thesis as well (figures 3.2 and 4.4). To characterise thrombi on fiber and protofibril levels, additional methodology, like for instance turbidimetry which was used by Piechocka *et al.*, has to be applied. While certainly interesting, if it is feasible in whole blood clots remains subject to further research.

Only one study specifically concerned with non-linear whole blood clot dynamics and fracture strain ($\gamma_{stiffest}$ in the terminology of this diploma thesis) could be identified.[44] $G'_{stiffest}$, $\tau_{stiffest}$, and $\gamma_{stiffest}$ measured by Riha *et al.* are nearly identical to data from the BL group.

Therefore it can be assumed that blood clots of healthy individuals disintegrate at shear deformation amplitudes of ≈70 %.[1] Interestingly, raising fibrinogen concentration doesn't yield blood clots more resistant to straining (as $\gamma_{stiffest}$ was about the same in sample groups).

5.2 Limitations

5.2.1 Sample preparation

Concentration of cellular blood components was affected by sample preparation. While erythrocyte concentration was only affected slightly, a great reduction of thrombocyte concentration was observed. This possibly resulted from premature thrombocyte activation, as laboratory reports indicated thrombocyte aggregates were found during haematological analysis. Thrombocyte activation is an delicate process and in this case, thrombocyte clumping propably happened because of direct addition of fibrinogen to the blood.

During preliminary tests, samples with increased fibrinogen concentration were also prepared by adding 1 mL of an fibrinogen stock solution at different concentrations. This resulted in additional haemodilution, which is known to interfere in the clotting process in vitro as well as in vivo.[56,57,58] Rheometric analysis of samples prepared by haemodilution showed great variation in G' development and experiments were not reproduceible.

So despite the effects on cellular components, the direct addition of fibrinogen was deemed feasible. One more finding supports this decision: On would respect reduced clot mechanical properties resulting from the reduction of thrombocyte concentration. It is however clearly demonstrated, that despite this reduction, clot

[1] Which equals 0.7 mm if a shearing gap with an 1 mm gap size is used

stiffness increases significantly as fibrinogen is added. We therefore hypothesise that thrombocyte concentration does play an minor role in development of clot stiffness compared to fibrinogen concentration.

5.2.2 Sedimentation of blood

In some MED and HIGH clots, macroscopic inhomogeneities were visible with separation of two layers: (1) a lower red layer with very weak tissue connectivity and (2) a top opaque layer. The top layer showed higher connectivity and macroscopic elasticity. Layer separation in the BL group wasn't observed. It is hypothesised that those layers correspond to a mainly cellular, respectively acellular or plasmatic phase which were not mixed adaequately during coagulation.

Triggered by those macroscopic observations, focus of SEM investigations shifted to analysis of 3D structure (see section 4.4), which also demonstrated sample inhomogeneity. It was hypothesised that increasing fibrinogen concentration results in samples with increased red blood cell sedimentation rate. Further literature research, the results of which are presented below, affirm this hypothesis.

Sedimentation can be defined as the settling of particles in the solvent. The settling entity in blood is not the individual erythrocyte, but rather erythrocyte aggregates. By aggregation, the number of sedimenting particles is reduced, whereas their size increases.[29] The kinetics of sedimentation are mostly depending on densities of RBC aggregates and plasma.

Under low shear flow or stasis, RBCs form so-called rouleauxs (resembling coin stacks) and/or branched round aggregates, which are easily dispersed by increasing shear stress.[59] As of this day, the underlying mechanisms of RBC aggregation are not fully understood. However, is was discovered that aggregation depends on (1) solvent characteristics as well as (2) intrinsic RBCs properties (aggregability). It is known that RBC aggregation does not occur in isotonic saline solutions, but only in solutions with fibrous macromolecules, the most important being fibrinogen.[29]

Probably the clinically most widely applied test for measuring RBC aggregation and sedimentation is the erythrocyte sedimentation rate (ESR): Whole blood is placed in

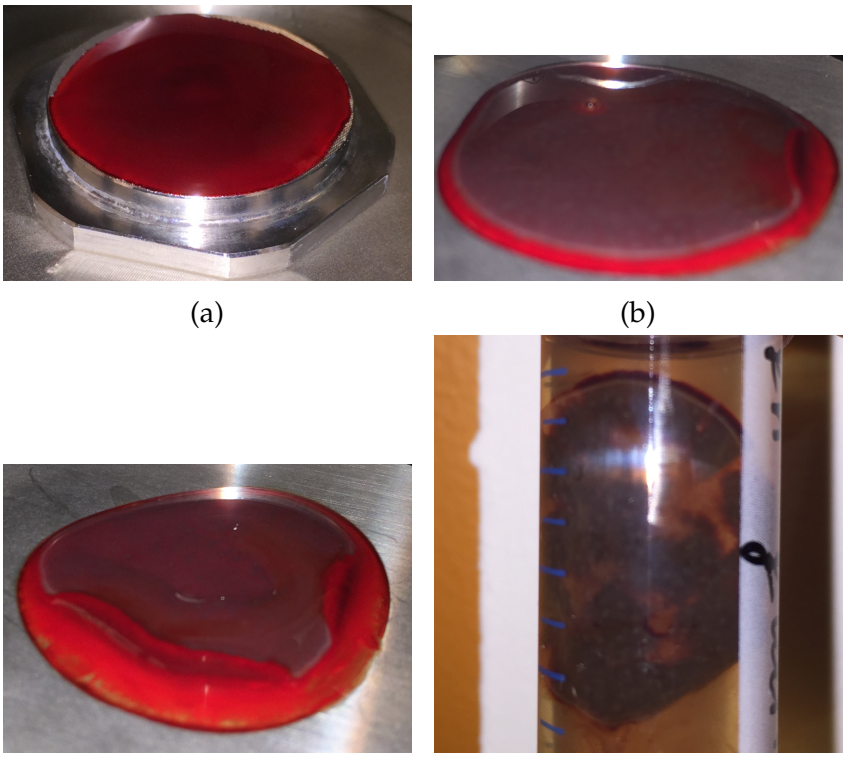

(a) (b)

(c) (d)

Figure 5.1: Selection of the blood clots produced in the rheometer after approximately 45 minutes. (a) shows a BL clot without any layer separation. All other clots are from the HIGH sample group. A separation into a lower cellular layer and a plasmatic upper layer is clearly visible.

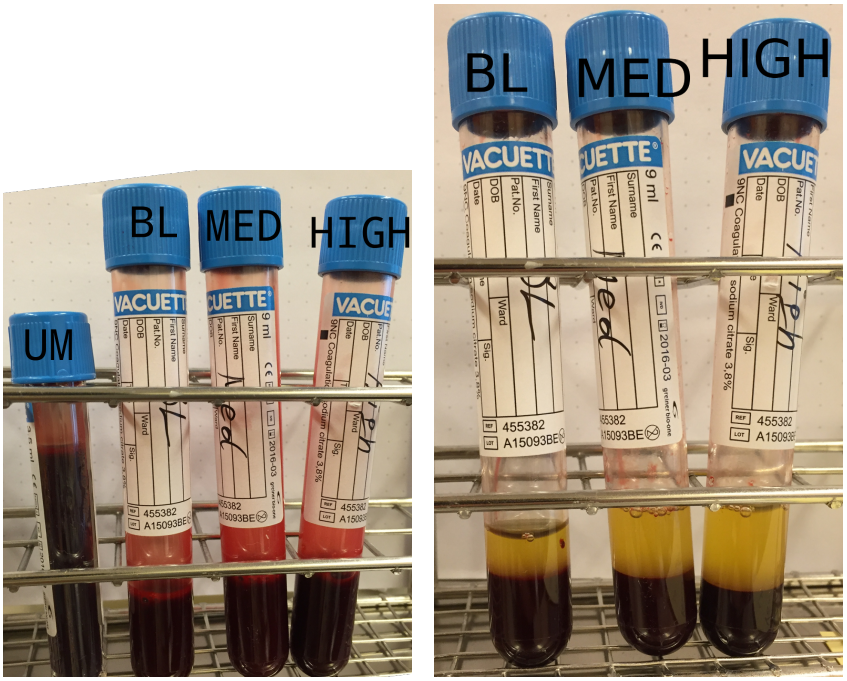

(a) (b)

Figure 5.2: Difference in blood sedimentation rate for the different blood sample groups. The containers in picture (a) were photographed immediately after careful mixing. Picture (b) was taken after 2 hours 15 minutes. Although this was not a standardised test for blood sedimentation rate, plasma fractions in MED and HIGH samples appear bigger, which corresponds to increased fibrinogen concentrations.

a standarised tube, mixed and then left alone for 1 hour. After this, the RBC fraction is measured and reported in mm. A more sophisticated approach is aggregrometry, which utilises photometry to provide so-called aggregation indices[60].

In this diploma thesis, increased fibrinogen concentration led to faster RBC aggregate formation and thus, sedimentation occured prior to fibrin network formation, which would have otherwise trapped the erythrocytes and therefore stopped the sedimentation.

The validity of rheometric measurements depends on sample homogeneity and sample sedimentation is a known issue in plate-plate rheometry.[4] Previous works — as to our knowledge — in the hemorheology of coagulation have not adressed sedimentation. In this diploma thesis, fibrinogen concentration was artificially increased, but fibrinogen increase is common in pathological conditions associated with inflammation or in malignant diseases. Further research is needed to establish if sedimentation and therefore clot inhomogeneities occur in patients with those conditions.

5.3 Ideas for further research

5.3.1 Sedimentation inhibition

As illustrated above, sedimentation possibly presents an important problem in rheometry – and also in other devices measuring viscoelastic clot parameters. By preventing RBC sedimentation, more accurate measurements would be possible. One possible idea is presented here:

Ficoll 70 kDa, a polysaccharide with a branched structure, has anti-aggregatory effects on RBCs and thereby increases the suspension stability of whole blood. Wong *et al.* have used Ficoll experimentally in order to enhance blood preservation when it's used for diagnostic tests.[61] However, in this study blood was diluted 1 : 3, which is a by far too high ratio for coagulation measurements. In order to limit the drastic effects of haemodilution introduced by Ficoll addition to blood samples, a minimal volume with high concentration has to be used.

5.3.2 Post-plateau development of clot viscoelasticity

Some measurements indicate that G' plateau of whole blood clots isn't as constant as previously thought, but rather begins to sink to a second, lower plateau. In this diploma thesis, detailed investigation into this phenomenon wasn't possible due to technical difficulties (mainly sample drying after prolonged measurment periods). This effect also occurs in other investigations using platelet rich plasma or whole blood and is therefore attributed to the presence of thrombocytes[62] and depletion of their metabolic energy reserves.[63]

5.3.3 Mechanical clot properties in coagulation disorders

In this diploma thesis blood was sampled only from healthy individuals. Increasing fibrinogen concentration serves only as a very limited in vitro model of pathological states. It is known that a wide number of common diseases influence the coagulation system: infection (sepsis), malignant diseases (i.e. breast cancer), trauma, hemophilia. Additionally, many patients regularly take medication either inhibiting cellular or plasmatic coagulation. Rheometric characterisation of patient with haemostatic abnormalities and/or anticoagulation intake would provide valuable information and could perhaps be used as monitoring device.

Bibliography

1. Versteeg, H. H., Heemskerk, J. W. M., Levi, M., *et al.* New fundamentals in hemostasis. *Physiological reviews* **93,** 327–58 (2013).
2. *Hemostasis and thrombosis: basic principles and clinical practice.* 6th (ed Marder, V.) (Lippincott Williams & Wilkins, 2013).
3. Williams, B., McNeil, J., Crabbe, A., *et al.* Practical Use of Thromboelastometry in the Management of Perioperative Coagulopathy and Bleeding. *Transfusion Medicine Reviews* **31,** 11–25 (2017).
4. Mezger, T. *Das Rheologie Handbuch: für Anwender von Rotations- und Oszillations-Rheometern* 5th ed. (Vincentz Network, Hannover, 2016).
5. MacFarlane, R. G. An Enzyme Cascade in the Blood Clotting Mechanism, and its Function as a Biochemical Amplifier. *Nature* **202,** 498–499 (May 1964).
6. Davie, E. W. & Ratnoff, O. D. Waterfall Sequence for Intrinsic Blood Clotting. *Science* **145,** 1310–1312 (Sept. 1964).
7. Monroe, D. M. & Hoffman, M. What does it take to make the perfect clot? *Arteriosclerosis, Thrombosis, and Vascular Biology* **26,** 41–48 (2006).
8. Hoffman, M. & Monroe, D. M. A cell-based model of hemostasis. *Thrombosis and Haemostasis* **85,** 958–965 (2001).
9. White, J. G. in *Platelets* 117–144 (Elsevier, 2013).
10. Shin, E.-K., Park, H., Noh, J.-Y., *et al.* Platelet Shape Changes and Cytoskeleton Dynamics as Novel Therapeutic Targets for Anti-Thrombotic Drugs. *Biomolecules & Therapeutics* **25,** 223–230 (May 2017).
11. Nurden, A. T., Pillois, X. & Wilcox, D. A. Glanzmann thrombasthenia: State of the art and future directions. *Seminars in Thrombosis and Hemostasis* **39,** 642–655 (2013).
12. Gachet, C. Antiplatelet drugs: which targets for which treatments? *Journal of Thrombosis and Haemostasis* **13,** S313–S322 (June 2015).
13. Carr, M. E. Development of platelet contractile force as a research and clinical measure of platelet function. *Cell biochemistry and biophysics* **38,** 55–78 (2003).

14. Lam, W. A., Chaudhuri, O., Crow, A., *et al.* Mechanics and contraction dynamics of single platelets and implications for clot stiffening. *Nature Materials* **10,** 61–66 (Jan. 2011).

15. Cines, D. B., Lebedeva, T., Nagaswami, C., *et al.* Clot contraction: Compression of erythrocytes into tightly packed polyhedra and redistribution of platelets and fibrin. *Blood* **123,** 1596–1603 (2014).

16. Weisel, J. W. & Litvinov, R. I. in *Fibrous Proteins: Structures and Mechanisms* (eds Parry, D. A. & Squire, J. M.) 405–456 (Springer International Publishing, 2017).

17. Chapin, J. C. & Hajjar, K. A. Fibrinolysis and the control of blood coagulation. *Blood Reviews* **29,** 17–24 (2015).

18. Mutch, N. & Booth, N. in *Hemostasis and thrombosis: Basic principles and clinical practice.* (ed Marder, V.) 6th. Chap. 20 (Lippincott Williams & Wilkins, 2012).

19. Lakes, R. S. *Viscoelastic Materials* (Cambridge University Press, 2009).

20. Hochleitner, G., Sutor, K., Levett, C., *et al.* Revisiting Hartert ' s 1962 Calculation of the Physical Constants of Thrombelastography. *Clinical and Applied Thrombosis/Haemostasis* **1** (2015).

21. Wufsus, A. R., Rana, K., Brown, A., *et al.* Elastic Behavior and Platelet Retraction in Low- and High-Density Fibrin Gels. *Biophysical Journal* **108,** 173–183 (Jan. 2015).

22. Litvinov, R. I. & Weisel, J. W. Fibrin mechanical properties and their structural origins. *Matrix Biology* (Aug. 2016).

23. Storm, C., Pastore, J. J., MacKintosh, F., *et al.* Nonlinear elasticity in biological gels. *Nature* **435,** 191–194 (2005).

24. Gardel, M. L. Elastic Behavior of Cross-Linked and Bundled Actin Networks. *Science* **304,** 1301–1305 (May 2004).

25. Semmrich, C., Larsen, R. J. & Bausch, A. R. Nonlinear mechanics of entangled F-actin solutions. *Soft Matter* **4,** 1675 (2008).

26. Broedersz, C. P., Kasza, K. E., Jawerth, L. M., *et al.* Measurement of nonlinear rheology of cross-linked biopolymer gels. *Soft Matter* **6,** 4120 (2010).

27. Sasaki, N. in *Viscoelasticity - From Theory to Biological Applications* (InTech, 2012).

28. Trautwein, A. X., Kreibig, U. & Hüttermann, J. *Physik für Mediziner, Biologen, Pharmazeuten* DT (Walter de Gruyter, Berlin, New York, Jan. 2008).

29. Baskurt, O. K. & Meiselman, H. J. Blood Rheology and Hemodynamics. *Seminars in Thrombosis and Hemostasis* **29,** 435–450 (2003).

30. Hyun, K., Wilhelm, M., Klein, C. O., *et al.* A review of nonlinear oscillatory shear tests: Analysis and application of large amplitude oscillatory shear (LAOS). *Progress in Polymer Science* **36,** 1697–1753 (Dec. 2011).

31. Bolliger, D. & Tanaka, K. A. Roles of thrombelastography and thromboelastometry for patient blood management in cardiac surgery. *Transfusion Medicine Reviews* **27,** 213–220 (Oct. 2013).

32. Van Kempen, T. *Rheological properties of the developing blood clot* PhD thesis (Technische Universiteit Eindhoven, 2015).

33. Tynngård, N., Lindahl, T., Ramström, S., *et al.* Effects of different blood components on clot retraction analysed by measuring elasticity with a free oscillating rheometer. *Platelets* **17,** 545–554 (2006).

34. Mace, H., Lightfoot, N., McCluskey, S., *et al.* Validity of Thromboelastometry for Rapid Assessment of Fibrinogen Levels in Heparinized Samples During Cardiac Surgery: A Retrospective, Single-center, Observational Study. *Journal of Cardiothoracic and Vascular Anesthesia* **30,** 90–95 (Jan. 2016).

35. Vucelic, D., Jesic, R., Jovicic, S., *et al.* Comparison of standard fibrinogen measurement methods with fibrin clot firmness assessed by thromboelastometry in patients with cirrhosis. *Thrombosis Research* **135,** 1124–1130 (June 2015).

36. Solomon, C., Cadamuro, J., Ziegler, B., *et al.* A comparison of fibrinogen measurement methods with fibrin clot elasticity assessed by thromboelastometry, before and after administration of fibrinogen concentrate in cardiac surgery patients. *Transfusion* **51,** 1695–1706 (Aug. 2011).

37. Shah, J. V. & Janmey, P. a. Strain hardening of fibrin gels and plasma clots. *Rheologica Acta* **36,** 262–268 (1997).

38. Scrutton, M. C., Ross-Murphy, S. B., Bennett, G. M., *et al.* Changes in clot deformability-a possible explanation for the epidemiological association between plasma fibrinogen concentration and myocardial infarction. *Blood Coagulation & Fibrinolysis* **5,** 719–723 (Oct. 1994).

39. Piechocka, I. K., Kurniawan, N. A., Grimbergen, J., *et al.* Recombinant fibrinogen reveals the differential roles of α - and γ -chain cross-linking and molecular heterogeneity in fibrin clot strain-stiffening. *Journal of Thrombosis and Haemostasis* **15,** 938–949 (May 2017).

40. Weisel, J. W. & Litvinov, R. I. Mechanisms of fibrin polymerization and clinical implications. *Blood* **121,** 1712–1719 (2013).

41. Litvinov, R. I. & Weisel, J. W. What Is the Biological and Clinical Relevance of Fibrin? *Seminars in Thrombosis and Hemostasis* **42,** 333–343 (2016).

42. Davenport, R. A. & Brohi, K. Cause of trauma-induced coagulopathy. *Current Opinion in Anaesthesiology* **29,** 212–219 (2016).

43. Kurniawan, N. A., Grimbergen, J., Koopman, J., *et al.* Factor XIII stiffens fibrin clots by causing fiber compaction. *Journal of Thrombosis and Haemostasis* **12,** 1687–1696 (Oct. 2014).

44. Riha, P., Wang, X., Liao, R., *et al.* Elasticity and fracture strain of whole blood clots. *Clinical hemorheology and microcirculation* **21,** 45–49 (1999).

45. Gersh, K. C., Nagaswami, C. & Weisel, J. W. Fibrin network structure and clot mechanical properties are altered by incorporation of erythrocytes. *Thrombosis and Haemostasis* **102,** 1169–1175 (Nov. 2009).

46. Wolberg, A. S. Plasma and cellular contributions to fibrin network formation, structure and stability. *Haemophilia* **16,** 7–12 (2010).

47. Tutwiler, V., Litvinov, R. I., Lozhkin, A. P., *et al.* Kinetics and mechanics of clot contraction are governed by the molecular and cellular composition of the blood. *Blood* **127,** 149–159 (2016).

48. Lam, W. A., Chaudhuri, O., Crow, A., *et al.* Mechanics and contraction dynamics of single platelets and implications for clot stiffening. *Nature Materials* **10,** 61–66 (Jan. 2011).

49. Kawasaki, J., Katori, N., Kodaka, M., *et al.* Electron Microscopic Evaluations of Clot Morphology During Thrombelastography. *Anesthesia & Analgesia* **99,** 1440–1444 (Nov. 2004).

50. Pretorius, E., Windberger, U. B., Oberholzer, H. M., *et al.* Comparative ultrastructure of fibrin networks of a dog after thrombotic ischaemic stroke. *The Onderstepoort journal of veterinary research* **77,** E1–4 (2010).

51. Silvain, J., Collet, J.-P., Guedeney, P., *et al.* Thrombus composition in sudden cardiac death from acute myocardial infarction. *Resuscitation* **113,** 108–114 (2017).

52. Clauss, A. Gerinnungsphysiologische Schnellmethode zur Bestimmung des Fibrinogens. Deutsch. *Acta Haematologica* **17,** 237–246 (1957).

53. R Core Team. *R: A Language and Environment for Statistical Computing* R Foundation for Statistical Computing (Vienna, Austria, 2017).

54. Solomon, C., Schöchl, H., Ranucci, M., *et al.* Comparison of fibrin-based clot elasticity parameters measured by free oscillation rheometry (ReoRox ®) versus thromboelastometry (ROTEM ®). *Scandinavian Journal of Clinical & Laboratory Investigation* **75,** 239–246 (May 2015).

55. Sølbeck, S., Windeløv, N. a., Bæk, N. H., *et al.* In-vitro comparison of free oscillation rheometry (ReoRox) and rotational thromboelastometry (ROTEM) in trauma patients upon hospital admission. *Blood Coagulation & Fibrinolysis* **23,** 688–92 (2012).

56. Gielen, C. L., Grimbergen, J., Klautz, R. J., *et al.* Fibrinogen reduction and coagulation in cardiac surgery. *Blood Coagulation & Fibrinolysis,* 1 (June 2015).

57. Tynngård, N., Berlin, G., Samuelsson, A., *et al.* Low dose of hydroxyethyl starch impairs clot formation as assessed by viscoelastic devices. *Scandinavian journal of clinical and laboratory investigation* **74,** 344–50 (2014).

58. Fries, D., Innerhofer, P., Reif, C., *et al.* The Effect of Fibrinogen Substitution on Reversal of Dilutional Coagulopathy: An In Vitro Model. *Anesthesia & Analgesia* **102,** 347–351 (Feb. 2006).

59. Fabry, T. L. Mechanism of erythrocyte aggregation and sedimentation. *Blood* **70,** 1572–6 (Nov. 1987).

60. Baskurt, O. K., Meiselman, H. J. & Kayar, E. Measurement of red blood cell aggregation in a "plate-plate" shearing system by analysis of light transmission. *Clinical hemorheology and microcirculation* **19,** 307–14 (Dec. 1998).

61. Wong, K. H. K., Sandlin, R. D., Carey, T. R., *et al.* The Role of Physical Stabilization in Whole Blood Preservation. *Scientific Reports* **6,** 21023 (Feb. 2016).

62. Lang, T., Toller, W., Gütl, M., *et al.* Different effects of abciximab and cytochalasin D on clot strength in thrombelastography. *Journal of thrombosis and haemostasis : JTH* **2,** 147–53 (Jan. 2004).

63. Evans, P., Hawkins, K., Lawrence, M., *et al.* Studies of whole blood coagulation by oscillatory shear, thromboelastography and free oscillation rheometry. *Clinical Hemorheology and Microcirculation* **38,** 267–277 (2008).

List of Figures